ORIGINAL ARTICLE

FISH and FISHERIES　WILEY

Spatio-temporal analyses of marine predator diets from data-rich and data-limited systems

Arnaud Grüss[1]　|　James T. Thorson[2]　|　Gemma Carroll[3,4]　|　Elizabeth L. Ng[5]　|
Kirstin K. Holsman[6]　|　Kerim Aydin[6]　|　Stan Kotwicki[7]　|　Hem N. Morzaria-Luna[8]　|
Cameron H. Ainsworth[9]　|　Kevin A. Thompson[10]

[1]School of Aquatic and Fishery Sciences, University of Washington, Seattle, WA, USA

[2]Habitat and Ecological Processes Research Program, Alaska Fisheries Science Center, National Marine Fisheries Service, NOAA, Seattle, WA, USA

[3]Institute of Marine Science, University of California Santa Cruz, Santa Cruz, CA, USA

[4]Environmental Research Division, Southwest Fisheries Science Center, National Marine Fisheries Service, National Oceanic and Atmospheric Administration, Monterey, CA, USA

[5]Quantitative Ecology and Resource Management, University of Washington, Seattle, WA, USA

[6]Resource Ecology and Fisheries Management Division, Alaska Fisheries Science Center, National Marine Fisheries Service, NOAA, Seattle, WA, USA

[7]Resource Assessment and Conservation Engineering Division, Alaska Fisheries Science Center, National Marine Fisheries Service, NOAA, Seattle, WA, USA

[8]Intercultural Center for the Study of Deserts and Oceans, Inc. (CEDO), Tucson, AZ, USA

[9]College of Marine Science, University of South Florida, St. Petersburg, FL, USA

[10]Florida Fish and Wildlife Conservation Commission, Fish and Wildlife Research Institute, St. Petersburg, FL, USA

Correspondence
Arnaud Grüss, School of Aquatic and Fishery Sciences, University of Washington, Box 355020, Seattle, WA 98105-5020, USA.
Email: gruss.arnaud@gmail.com

Funding information
The David and Lucile Packard Foundation, Grant/Award Number: 2019-69067

Abstract

Accounting for variation in prey mortality and predator metabolic potential arising from spatial variation in consumption is an important task in ecology and resource management. However, there is no statistical method for processing stomach content data that accounts for fine-scale spatio-temporal structure while expanding individual stomach samples to population-level estimates of predation. Therefore, we developed an approach that fits a spatio-temporal model to both prey-biomass-per-predator-biomass data (i.e. the ratio of prey biomass in stomachs to predator weight) and predator biomass survey data, to predict "predator-expanded-stomach-contents" (PESCs). PESC estimates can be used to visualize either the annual landscape of PESCs (spatio-temporal variation), or can be aggregated across space to calculate annual variation in diet proportions (variation among prey items and among years). We demonstrated our approach in two contrasting scenarios: a data-rich situation involving eastern Bering Sea (EBS) large-size walleye pollock (*Gadus chalcogrammus*, Gadidae) for 1992–2015; and a data-limited situation involving West Florida Shelf red grouper (*Epinephelus morio*, Epinephelidae) for 2011–2015. Large walleye pollock PESC was predicted to be higher in very warm years on the Middle Shelf of the EBS, where food is abundant. Red grouper PESC was variable in north-western Florida waters, presumably due to spatio-temporal variation in harmful algal bloom severity. Our approach can be employed to parameterize or validate diverse ecosystem models, and can serve to address many fundamental ecological questions, such as providing an improved understanding of how climate-driven changes in spatial overlap between predator and prey distributions might influence predation pressure.

KEYWORDS

diet proportions, Poisson-link delta model, predation pressure, predator-expanded-stomach-contents, spatio-temporal model, stomach content data

1 | INTRODUCTION

Trophic interactions play a fundamental role in shaping the behaviour (Catano, Shantz, & Burkepile, 2014; Charnov, 1976), spatial distribution (Hunsicker, Ciannelli, Bailey, Zador, & Stige, 2013; Selden, Batt, Saba, & Pinsky, 2018) and population dynamics (Daskalov, 2002; Lilly, Parsons, & Kulka, 2000) of fish species. For this reason, accurately measuring spatial and temporal variation in consumption is an important area of research in fisheries ecology (Baker, Buckland, & Sheaves, 2014). However, traditional approaches to estimating diet compositions and consumption usually do not account for fine-scale spatio-temporal structure in predator–prey dynamics. This can mask important fine-scale patterns (e.g. Buckley, Ortiz, Kotwicki, & Aydin, 2016; Glaser, 2010) and can lead to biases in estimating predation pressure at the population level (Binion-Rock, Reich, & Buckel, 2018; Reum, Blanchard, Holsman, Aydin, & Punt, 2019). Advances in quantitative methods for analysing spatially explicit diet data can provide new and more accurate insights into trophic dynamics in marine ecosystems and may strengthen efforts towards ecosystem-based fisheries management (EBFM; Patrick & Link, 2015).

The contribution of different prey categories to predators' diet by weight, generally referred to as "diet proportions," is the most popular metric used in fisheries studies of trophic interactions (Baker et al., 2014; Elliott & Persson, 1978; Liao, Pierce, & Larscheid, 2001; Livingston et al., 2017). Diet proportions are typically determined from analyses of fish stomachs collected by fisheries-independent surveys or obtained from fishers (Ainsworth, Kaplan, Levin, & Mangel, 2010; Glaser, 2010; Livingston et al., 2017; Moriarty, Essington, & Ward, 2017). Importantly, diet proportion estimates are needed to parameterize the diet matrices of most of the ecosystem modelling platforms that are instrumental in advancing EBFM (e.g. dynamic multispecies models; Holsman, Ianelli, Aydin, Punt, & Moffitt, 2016; Kinzey & Punt, 2009; Livingston & Jurado-Molina, 2000; Ecopath with Ecosim (EwE); Christensen & Walters, 2004; Atlantis; Fulton, Parslow, Smith, & Johnson, 2004).

Fisheries studies have generally employed simple methods for estimating diet proportions from stomach content data, including simple and weighted averages of sampled diet compositions (e.g. Chagaris, Mahmoudi, Walters, & Allen, 2015; Geers, Pikitch, & Frisk, 2016; Liao et al., 2001; Livingston et al., 2017; Nielsen, Johnson, & American Fisheries Society, 1983), or they have relied largely on expert opinion (e.g. Arreguín-Sánchez, Valero-Pacheco, & Chávez, 1993; Walters, Martell, Christensen, & Mahmoudi, 2008). To obtain simple average estimates of diet compositions, analysts determine the contribution of prey items to the predator's diet for all analysed stomachs and then estimate the mean contributions of prey items to the predator's diet across all stomachs (Hyslop, 1980). The weighted average method is similar to the simple average method, except that some individual stomachs are given more weight in calculations, based, for example, on where and how the stomachs were collected (Sagarese et al., 2016). The simple and weighted average methods have several flaws. Notably, when applied to a small number of samples (a common situation in fish diet studies), these methods tend to

overestimate the proportion of minor prey in a predator's diet and to underestimate the importance of major prey, particularly when prey items are not pooled into broad taxonomic groups (Ainsworth et al., 2010; Masi, Ainsworth, & Chagaris, 2014; Tarnecki, Wallace, Simons, & Ainsworth, 2016). Moreover, the simple and weighted average methods can generate biased diet proportion estimates if they do not take into account opportunistic or rare predation events, or if stomach samples are not pooled at the sample event level when there is a lack of independence among the samples collected within the same sampling event (Livingston et al., 2017; Masi et al., 2014; Sagarese et al., 2016).

Despite decades of research on fish diet patterns (Baker et al., 2014; Hynes, 1950; Hyslop, 1980; Pierce & Boyle, 1991), statistical models for estimating diet proportions have only recently been developed. Statistical models offer several advantages, including formal model selection (e.g. using Akaike's information criterion), the ability to combine data coming from different sources (e.g. recently collected stomach samples, diet composition information available online, expert opinion) in a rigorous way and the potential to account for the lack of independence among the samples collected within the same sampling event when stomach samples are not pooled at the sample event level (Ainsworth et al., 2010; Moriarty et al., 2017). Importantly, statistical models that estimate diet proportions are able to directly quantify the uncertainty

associated with diet proportion estimates (Ainsworth et al., 2010; Reum et al., 2019; Sagarese et al., 2016), and allow for the generation of input sample sizes that are useful for multispecies stock assessments (Thorson, 2014; Thorson & Haltuch, 2018). Stock assessments that rely on compositional data need an input sample size that approximates the estimated imprecision for proportions (Thorson, 2014; Thorson, Johnson, Methot, & Taylor, 2017). These input sample sizes are typically used in stock assessments as starting points or upper bounds for weighting compositional data relative to abundance-index data (Francis, 2011; Kinzey & Punt, 2009; Thorson et al., 2017).

Ainsworth et al. (2010) developed an approach relying on multiple data sources, which fits a Dirichlet model to bootstrapped diet composition data (hereafter referred to as the "Ainsworth method"). More specifically, the Ainsworth method consists of: (a) compiling a large diet composition dataset that combines stomach content data with information from the literature and online databases (e.g. FishBase; Froese & Pauly, 2019); (b) bootstrapping the large diet composition dataset to produce likelihood profiles; (c) fitting the bootstrapped data to a Dirichlet distribution, which is a multivariate generalization of the Beta distribution (Douma & Weedon, 2019); and (d) employing the maximum likelihood estimates (MLEs) from the marginal Beta distributions of the Dirichlet model to define mean diet proportions for each predator of interest, and using the standard errors of these distributions to generate confidence intervals. The Ainsworth method has been employed and further developed in Masi et al. (2014), Sagarese et al. (2016), Tarnecki et al. (2016), Morzaria-Luna, Ainsworth, Tarnecki, and Grüss (2018) and Reum et al. (2019).

The Ainsworth method must resolve a large number of covarying prey items through the use of the multivariate Dirichlet distribution. Thus, the Ainsworth method is less influenced by rare feeding events than the simple average method and is, therefore, convenient for working with the small diet composition datasets that are typically available to fisheries analysts (Ainsworth et al., 2010; Tarnecki et al., 2016). Moreover, the confidence intervals estimated by the Ainsworth method provide information about fish diet variability, data quality and uncertainty about rare feeding events (Masi et al., 2014; Morzaria-Luna et al., 2018). However, as noted by Moriarty et al. (2017), an issue with the Ainsworth method is that it cannot be directly employed (i.e. a workaround is needed) if any of the entries of the dataset at hand are associated with diet proportions that are exactly 0 or 1, because these values are outside the support of the Dirichlet distribution.

Moriarty et al. (2017) implemented a likelihood-based mixture model for estimating diet proportions (hereafter referred to as the "Moriarty method"). The Moriarty method uses a mixture of Bernoulli, Gamma and Beta models to deal with the specific cases where the proportion of a prey item in sampled stomachs is 0, ranges between 0 (exclusive) and 1 (exclusive), or is 1. Thus, the sophistication of the Moriarty method addresses two important challenges often faced with fish stomach content data: extreme events in stomach content biomass; and covariance between stomach content biomass and observed diet proportions. The Moriarty method generally demonstrates better accuracy and precision than the simple or weighted average method when applied to simulated or real data, and is more robust to outliers (Moriarty et al., 2017).

While the Ainsworth and Moriarty methods represent large improvements over the simple and weighted average methods, they do not take into account spatial patterns of fish diet. This is despite the fact that trophic interactions can vary widely within a given marine region (Buckley et al., 2016; Glaser, 2010; Tarnecki et al., 2016). To address this issue, Binion-Rock et al. (2018) designed a spatially explicit kernel density method, which takes spatial structure (i.e. spatial autocorrelation) into account to determine diet proportions. The spatially explicit kernel density method was found to be more precise than a simple cluster-based method (Binion-Rock et al., 2018). Yet, Binion-Rock et al. (2018) noted that, for data from long-tailed distributions, the bandwidth (i.e. the width of the kernel) that defines the amount of spatial smoothing is difficult to adjust to avoid erroneous noise in the tails of the estimates. Moreover, while the spatially explicit kernel density method explicitly considers unmeasured variation in fish diet composition that is stable over time ("spatial variation"), it does not take into account unmeasured variation in diet composition that changes between years ("spatio-temporal variation"), which can be large for many fish populations (e.g. Buckley et al., 2016; Kaplan et al., 2019).

In this study, we develop a novel spatio-temporal statistical modelling approach to analysing diet data, which takes into account both spatial and spatio-temporal structure at a fine scale. Our approach primarily differs from the Ainsworth, Moriarty and spatially explicit kernel density methods in that it does not fit a model to diet composition data in order to generate diet proportion estimates. Rather, our approach fits a model to both prey-biomass-per-predator-biomass data (i.e. the ratio of prey biomass in stomachs to predator weight) and predator biomass catch rate data, to predict "predator-expanded-stomach-contents" (the product of prey-biomass-per-predator-biomass, predator biomass per unit area and surface area). The predator-expanded-stomach-contents predicted by our model and their standard errors can be used to calculate diet proportions and their associated standard errors, as well as input sample sizes that are useful for multispecies stock assessments. In addition, as our model is spatio-temporal, its predictions can be used to explore spatial and temporal patterns in predator-expanded-stomach-contents. Here, we demonstrate our spatio-temporal modelling approach to estimating predator-expanded-stomach-contents and diet proportions in two contrasting situations: a data-rich situation, for large (55+ cm) walleye pollock (*Gadus chalcogrammus*, Gadidae) of the eastern Bering Sea; and a (more common) data-limited situation, for the red grouper (*Epinephelus morio*, Epinephelidae) population of the West Florida Shelf region. We also compare the diet proportions (and their associated standard errors) predicted by our spatio-temporal modelling approach to those predicted by a non-spatial equivalent of our approach and the Ainsworth and simple average methods.

2 | METHODS

2.1 | Model overview

Our spatio-temporal modelling approach primarily differs from previous methods to estimating diet proportions in that our spatio-temporal model is not fitted to diet composition data, but rather to prey-biomass-per-predator-biomass data (in units kilograms of prey per kilogram of predator, as measured from stomach-content samples) and predator biomass catch rate data (in units kilograms of predator per km^2, as measured from monitoring programmes). Stomach content analysis provides biomass data (in units kilograms) for individual prey items (e.g. fish, crabs, shrimps and other prey) found in predator stomachs. Moreover, when stomach content analysis is performed, the weight of individual predator fishes (in units kilograms) is typically recorded or estimated from predator length. Thus, fisheries analysts typically have available both biomass data for several prey items and predator weight data. We define "prey-biomass-per-predator-biomass" for a given prey item as the ratio of biomass for that prey item to predator weight. In parallel, monitoring programmes generally provide biomass catch rate data for the fish predators of interest. Our spatio-temporal model uses both prey-biomass-per-predator-biomass data for several prey items coming from stomach content analysis and predator biomass catch rate data collected by monitoring programmes to estimate: (a) predator-expanded-stomach-contents (PESC) for the different prey items (the relative biomasses of the different prey items eaten by the predator population; in units kilograms), and (b) diet proportions (the proportions of the different prey items in the diet of the predator). Because our model is spatio-temporal, both the prey-biomass-per-predator-biomass and predator biomass catch rate data provided to our model must be georeferenced.

Our spatio-temporal modelling approach can be divided into five steps. First, if several stomachs of the predator of interest are collected at a given location s in a given year t, then the average prey-biomass-per-predator-biomass for each prey item p at location s in year t is calculated. This step is implemented because individual predator stomachs collected in the same sampling event (e.g. coming from the same haul) are generally not independent samples (Binion-Rock et al., 2018; Moriarty et al., 2017; Nielsen et al., 1983). Second, a spatio-temporal model is fitted to prey-biomass-per-predator-biomass and predator biomass catch rate data collected at different locations in different years. The spatio-temporal model predicts the relative biomass of prey item p eaten by the predator (i.e. PESC for prey item p) at each location s and in each year t. Third, for each year t, the estimated PESCs are standardized by total PESC across prey items to determine the proportion of each prey item p in the diet of the predator in year t. Fourth, the variance of diet proportions is estimated. Fifth, a multinomial input sample size that approximates the estimated imprecision for proportions is calculated; this sample size can be used to "weight" the diet proportion estimates in a subsequent multispecies stock assessment model that treats them as following a multinomial distribution (Thorson, 2014; Thorson et al.,

2017). All five steps of our spatio-temporal modelling approach are implemented using R package "VAST" release number 3.0.0 (Thorson, 2019).

To estimate prey-biomass-per-predator-biomass for the different prey items and predator biomass-density, our model relies on the Poisson-link delta modelling framework (Thorson, 2018). Below, we describe in detail how the Poisson-link delta modelling framework predicts predator biomass-density from predator biomass catch rate data. Prey-biomass-per-predator-biomass is predicted at the different locations in the different years from prey-biomass-per-predator-biomass data in a similar way.

2.2 | Model details

2.2.1 | Poisson-link delta modelling framework

For simplicity, let us imagine that only predator biomass catch rate data are provided to the spatio-temporal model. From these biomass catch rate data collected at different locations in different years, the Poisson-link delta modelling framework estimates numbers-density (in units numbers per km^2) at each location s and in each year t, $n(s, t)$, and biomass-per-individual (in units kilograms per number) at each location s and in each year t, $w(s, t)$. Multiplying these two quantities together gives biomass-density (in units kilograms per km^2) at each location s and in each year t, $d(s, t$; Thorson, 2018).

Biomass-density is also given by the product of probability of encounter ρ and expected biomass-density given encounter (referred to as "positive catch rate"; in units kilograms per km^2) r (Lo, Jacobson, & Squire, 1992). The Poisson-link delta modelling framework assumes that the spatial distribution of individuals in the neighbourhood of sampling is random, such that the probability of encountering at least one individual follows a Poisson distribution with intensity equal to local numbers-density times the area sampled (Thorson, 2018):

$$\rho(i) = 1 - \exp\left(-a_i n\left(s_i, t_i\right)\right) \tag{1}$$

where a_i is the area sampled for sample i (in km^2). Then, as the product of probability of encounter ρ and positive catch rate r is equal to expected biomass-density and is also equal to the product of numbers-density n and biomass-per-individual w, it is possible to calculate positive catch rate as:

$$r(i) = \frac{n\left(s_i, t_i\right)}{\rho(i)} w\left(s_i, t_i\right) \tag{2}$$

Given the above, the probability of the biomass catch rate data $b(i)$ is calculated as:

$$\Pr(b(i) = B) = \begin{cases} 1 - \rho(i) & \text{if } B = 0 \\ \rho(i) \times g\left(B | r(i), \sigma_b^2\right) & \text{if } B > 0 \end{cases} \tag{3}$$

where $g\left(B|r(i),\sigma_b^2\right)$ is the Gamma probability density function for unexplained variation in $r(i)$; and σ_b^2 is residual biomass catch rate variation.

Numbers-density and biomass-per-individual are estimated as:

$$\log\left(n\left(s_i,t_i\right)\right) = \beta_n\left(t_i\right) + \omega_n\left(s_i\right) + \varepsilon_n\left(s_i,t_i\right)$$
$$\log\left(w\left(s_i,t_i\right)\right) = \beta_w\left(t_i\right) + \omega_w\left(s_i\right) + \varepsilon_w\left(s_i,t_i\right) \tag{4}$$

where $\beta_n\left(t_i\right)$ and $\beta_w\left(t_i\right)$ are intercepts for year t_i associated with sample i, which are both estimated as fixed effects; $\omega_n\left(s_i\right)$ and $\omega_w\left(s_i\right)$ represent spatial variation and are both estimated as random effects; and $\varepsilon_n\left(s_i,t_i\right)$ and $\varepsilon_w\left(s_i,t_i\right)$ represent spatio-temporal variation and are both estimated as random effects. Equation (4) could also include catchability and environmental covariates, but we do not consider this option here and leave it for future research (see the Section 4).

The spatial and spatio-temporal variation terms are all assumed to follow a multivariate normal distribution:

$$\omega_n \sim MVN\left(0,\sigma_{n\omega}^2 \mathbf{R}\left(\kappa_n\right)\right)$$
$$\varepsilon_n(t) \sim MVN\left(0,\sigma_{n\varepsilon}^2 \mathbf{R}\left(\kappa_n\right)\right)$$
$$\omega_w \sim MVN\left(0,\sigma_{w\omega}^2 \mathbf{R}\left(\kappa_w\right)\right) \tag{5}$$
$$\varepsilon_w(t) \sim MVN\left(0,\sigma_{w\varepsilon}^2 \mathbf{R}\left(\kappa_w\right)\right)$$

where $\mathbf{R}\left(\kappa_n\right)$ is the correlation among locations as a function of decorrelation distance κ_n; $\mathbf{R}\left(\kappa_w\right)$ is the correlation among locations as a function of decorrelation distance κ_w; $\sigma_{n\omega}^2$ and $\sigma_{w\omega}^2$ are the estimated pointwise variances of the spatial variation in numbers-density and biomass-per-individual, respectively; and $\sigma_{n\varepsilon}^2$ and $\sigma_{w\varepsilon}^2$ are the estimated pointwise variances of the spatio-temporal variation in numbers-density and biomass-per-individual, respectively. The $\mathbf{R}$ terms are calculated from a Matérn function taking geometric anisotropy (the fact that autocorrelation between locations may vary with both distance and direction) into account (Thorson & Haltuch, 2018; Thorson, Shelton, Ward, & Skaug, 2015). Gaussian Markov random fields are employed to estimate all spatial and spatio-temporal variation terms (Grüss, Thorson, et al., 2017; Thorson et al., 2015). All spatial and spatio-temporal variation terms are also specified to have a standard deviation of 1.0, which enables the parameters $\sigma_{n\omega}^2$, $\sigma_{n\varepsilon}^2$, $\sigma_{w\omega}^2$ and $\sigma_{w\varepsilon}^2$ to be identifiable and interpreted as the standard deviation of a given spatial or spatio-temporal process (Thorson & Haltuch, 2018).

Ultimately, the n and w estimates are multiplied together to obtain an estimate of predator biomass-density d (in units kilograms per km^2). When prey-biomass-per-predator-biomass data are provided to the spatio-temporal model instead of biomass catch rate data, the processes and equations (Equations 1–5) are similar, except that the product of the n and w estimates gives an estimate of prey-biomass-per-predator-biomass α (in units kilograms of prey per kilogram of predator). However, in effect, our spatio-temporal model is a multivariate model where both predator biomass catch rate and prey-biomass-predator-biomass data are inputs used to estimate separately, but simultaneously, predator biomass-density d and prey-biomass-per-predator-biomass α. Therefore, in effect, our

spatio-temporal model relies on equivalents of Equations (1–5) where the variables and parameters (except the area sampled a and the correlations among locations $\mathbf{R}\left(\kappa_n\right)$ and $\mathbf{R}\left(\kappa_w\right)$) are also indexed by "category," where category $c=1$ is the predator of interest and categories $c\geq 2$ are the prey items. When using a multivariate model that includes both predator biomass catch rate and prey-biomass-predator-biomass data, we assume that all spatial and spatio-temporal terms are independent for every category c; future research could relax this assumption to explore, for example density-dependent PESC (where stomach contents and/or prey selection depends on predator density).

2.2.2 | Parameter estimation

The estimation of fixed effects for the different "categories" (where category $c=1$ is the predator of interest and categories $c\geq 2$ are the prey items), namely $\beta_n(c,t)$, $\beta_w(c,t)$, $\sigma_{n\omega}^2(c)$, $\sigma_{n\varepsilon}^2(c)$, $\sigma_{w\omega}^2(c)$, $\sigma_{w\varepsilon}^2(c)$ and $\sigma_b^2(c)$, is accomplished by identifying the parameter values maximizing the marginal log-likelihood. First, the Laplace approximation implemented by R package "TMB" (Kristensen, Nielsen, Berg, Skaug, & Bell, 2016) is used to calculate the marginal log-likelihood via an approximation of the integral across all random effects. By using automatic differentiation, TMB efficiently calculates the matrix of second derivatives (which is employed by Laplace approximation), as well as the gradient of the Laplace approximation (which is employed when maximizing the fixed effects). Through the maximization of the marginal log-likelihood given the MLEs of the fixed effects, TMB predicts all random effects. Additionally, for computational efficiency, the probability of the random effects is approximated using the stochastic partial differential equation method (Lindgren, Rue, & Lindström, 2011). The bias-correction estimator developed in Thorson and Kristensen (2016) is utilized to correct for the "retransformation bias" when any derived quantity involving a non-linear transformation of random effects is predicted. Finally, the generalized delta method implemented in TMB is employed to compute the standard errors of all fixed and random effects, as well as the standard errors of derived quantities (Kass & Steffey, 1989).

2.2.3 | Estimation of predator-expanded-stomach-contents

After values have been estimated for the fixed and random effects, the spatio-temporal model uses these values to predict prey-biomass-per-predator-biomass for each prey item p (in units kilograms of prey per kilogram of predator) at each location s and in each year t, $\hat{\alpha}_p(s,t)$, and the biomass-density of the predator of interest q (in units kilograms per km^2) at each location s and in each year t, $\hat{d}_q(s,t)$. Subsequently, the relative biomass of each prey item p eaten by predator q in each year t (i.e. PESC for each prey item p in each year t; in units kilograms), $\hat{B}_p(t)$, is calculated as:

$$\hat{B}_p(t) = \sum_{s=1}^{n_s}\left(a_s \times \hat{d}_q(s,t) \times \hat{\alpha}_p(s,t)\right) \tag{6}$$

where n_s is the total number of locations in the study spatial domain, and a_s is the surface area associated with location s (in km^2).

2.2.4 | Estimation of diet proportions and input sample sizes

The proportion of each prey item p in the diet of the predator of interest in year t can then be computed from PESCs as:

$$\hat{P}_p(t) = \frac{\hat{B}_p(t)}{\sum_{p=1}^{n_p} \hat{B}_p(t)} \tag{7}$$

where n_p is the total number of prey items considered. The variance of each estimated diet proportion, $SE\left[\hat{P}_p(t)\right]^2$, is approximated as Thorson and Haltuch (2018):

$$SE\left[\hat{P}_p(t)\right]^2 = \frac{\hat{B}_p(t)^2}{\left(\sum_{p=1}^{n_p} \hat{B}_p(t)\right)^2}$$

$$\left[\frac{SE\left[\hat{B}_p(t)\right]^2}{\hat{B}_p(t)^2} - 2\frac{SE\left[\hat{B}_p(t)\right]^2}{\hat{B}_p(t)\sum_{p=1}^{n_p}\hat{B}_p(t)} + \frac{\sum_{p=1}^{n_p}SE\left[\hat{B}_p(t)\right]^2}{\left(\sum_{p=1}^{n_p}\hat{B}_p(t)\right)^2}\right] \tag{8}$$

For any combination of prey item p and year t for which there is no encounter, it is specified that $\hat{B}_p(t) = SE\left[\hat{P}_p(t)\right]^2 = 0$. This variance approximation is used to maintain computational efficiency (i.e. separable computations across categories).

From estimates of diet proportions and their variance, it is then possible to calculate the input sample size, $\hat{\tau}(t)$, which approximates the estimated imprecision for diet proportions (Thorson, 2014; Thorson et al., 2017). This input sample size can be employed in multispecies stock assessments relying on diet proportion data as starting points or upper bounds for weighting the diet proportion data relative to abundance-index data (Francis, 2011; Kinzey & Punt, 2009; Thorson et al., 2017). The input sample size $\hat{\tau}(t)$ is calculated as Thorson and Haltuch (2018):

$$\hat{\tau}(t) = \text{median}_{p=1,\dots,n_p}\left\{\frac{\hat{P}_p(t)\left(1-\hat{P}_p(t)\right)}{SE\left[\hat{P}_p(t)\right]^2}\right\} \tag{9}$$

2.3 | Data-rich case-study

We first carry out a demonstration of our spatio-temporal modelling approach in a data-rich situation, for large (55 + cm) walleye pollock of the eastern Bering Sea (EBS), a marine region located off Alaska (Figure 1a). For this demonstration, we rely on two sources of data for the period 1992–2015: (a) large walleye pollock biomass catch rate data (in kg per km^2) collected during the standardized EBS bottom trawl surveys conducted by the Alaska Fisheries Science Center (AFSC; Stauffer, 2004), and (b) large walleye
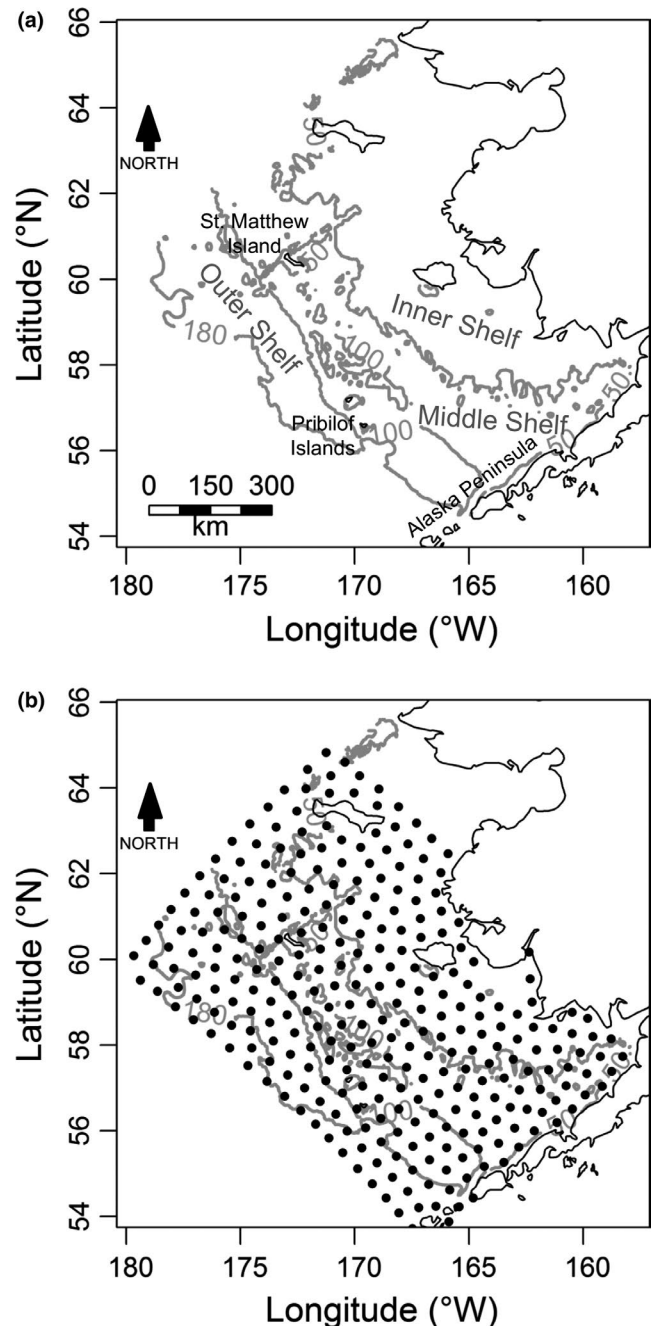
FIGURE 1 (a) Map of the eastern Bering Sea off Alaska. Depth contours are labelled in 50-, 100- and 180-m contours. Important features are labelled and include the Inner Shelf (0–50 m), Middle Shelf (50–100 m) and Outer Shelf (100–180 m), the Alaska Peninsula, the Pribilof Islands and St. Matthew Island. (b) Spatial distribution of the "knots" specified to approximate all spatial and spatio-temporal variation terms for the eastern Bering Sea. Depth contours are labelled in the background for reference in 50-, 100- and 180-m contours

pollock stomach content data from the AFSC's Groundfish Trophic Interactions Database (Livingston et al., 2017; Appendix S1). The standardized EBS bottom trawl surveys collect fish samples over the entire EBS shelf region in June–September each year, using a fixed-station sampling scheme involving approximately 376 stations

each year on a 20 km × 20 km grid (including areas with more dense sampling near significant islands; Stauffer, 2004). At each of the stations sampled by the standardized EBS bottom trawl surveys, species-specific length stratification is employed to select some of the sampled fish for stomach content analyses to populate the AFSC's Groundfish Trophic Interactions Database (Livingston et al., 2017). For example, in the case of walleye pollock, four length categories are considered: 1–24 cm, 25–39 cm, 40–54 cm and 55+ cm. Due to this sampling stratification, we focus only on a specific length category in this study, namely the large (55+ cm) walleye pollock length category. Other than the stomach sampling length stratification, the rationale behind focusing on large (55+ cm) walleye pollock is that there is an interesting shift from more pelagic prey to more demersal prey, including a greater proportion of fish, in walleye pollock between 50 and 60 cm (Livingston et al., 2017). Future applications of our approach to analysing diet data could conduct the same analyses for other pollock length categories, including the 40–54 cm length category, which comprises a larger portion of the EBS walleye pollock population, or both the 55–62 cm and 63+ cm length categories, as 63+ cm walleye pollocks appear to be distributed more on the Middle-Inner shelf of the EBS than 55–62 cm fish walleye pollocks that are more generally found in the Outer-Middle shelf (Barbeaux, 2018). Also, future applications of our approach could conduct separate analyses for several individual walleye pollock length categories (e.g. 1–24 cm, 25–39 cm, 40–54 cm, 55–62 cm and 63+ cm walleye pollocks) and then aggregate PESC across length categories. There is a large number of entries in the AFSC's Groundfish Trophic Interactions Database, and prey items are often identified to the species, genus or family levels. However, in this study, we only considered the six prey items that are most frequently encountered in large walleye pollock stomachs (amphipods, copepods, Euphausiacea, fish, Mysidacea and shrimps), as well as a seventh item that aggregates all other prey found in large walleye pollock stomachs which is referred

to as "other prey" (Table 1; Livingston et al., 2017). The original dataset from the AFSC's Groundfish Trophic Interactions Database, which we retrieved from NOAA Fisheries (2019), had 52,047 prey entries associated with a biomass value (in g), for a total of 19,529 large walleye pollock collected in 3,399 hauls. After reorganizing the dataset around the seven prey items of interest (Appendix S1), we had a total of 43,347 entries for 18,497 large walleye pollock stomachs collected in 3,360 hauls. The number of entries reduced to 9,843 after averaging the biomasses for each prey item in each haul (first step of our spatio-temporal modelling approach). At this stage, some hauls had no entry for some of the prey items, and we treated these instances as an observation of zero biomass for those prey items in those hauls, resulting in a final dataset with a total of 3,360 × 7 = 23,520 entries (Figure S1). To obtain prey-biomass-per-predator-biomass data (in g per g of predator), we used the walleye pollock weights (in g) calculated from a long-term average length–weight regression as part of AFSC's Groundfish Trophic Interactions Database.

In the spatio-temporal model for EBS large walleye pollock, we defined all spatial and spatio-temporal variation terms over a fixed spatial domain Ω ($s \in \Omega$) as being piecewise constant, for computational efficiency. To approximate all the spatial and spatio-temporal variation terms defined over domain Ω, we specified 300 "knots" uniformly distributed over the 20 km × 20 km spatial grid for the EBS (Figure 1b). The values of all spatial and spatio-temporal variation terms were tracked at each knot by the spatio-temporal model (Shelton, Thorson, Ward, & Feist, 2014). Consequently, the value of a spatial or spatio-temporal variation term at a given location $s \in \Omega$ was the value of the spatial or spatio-temporal variation term at the knot that was the closest to location s. The locations of the 300 knots were held fixed during model parameter estimation. We chose a total of 300 knots, because this number of knots offered a good compromise between accuracy and computational speed.

TABLE 1 Prey of large (55+ cm) eastern Bering Sea walleye pollock (*Gadus chalcogrammus*, Gadidae) considered in this study

Prey item	Components
Amphipods	Amphipoda, Capreillidea, Gammaridea, Hyperiidea
Copepods	Copepoda
Euphausiacea	Euphausiacea
Fish	Agonidae, Ammodytidae, *Atheresthes evermanni*, *Atheresthes stomias*, bathylagid, Clupeoidei, cottid, Cyclopteridae, flatfish, Gadidae, *Gadus chalcogrammus*, *Gadus macrocephalus*, *Hippoglossoides elassodon*, *Hippoglossoides robustus*, *Hippoglossus stenolepis*, *Lepidopsetta polyxystra*, *Lepidopsetta* spp., *Limanda aspera*, non-teleost fish, osmerid, Pholidae, *Pleuronectes quadrituberculatus*, *Reinhardtius hippoglossoides*, rockfish, Salmonidae, Stichaeidae, teleost, *Trichodon trichodon*, Zoarcoidae
Mysidacea	Mysidacea
Shrimps	Crangonidae, Hippolytidae, Pandalidae, shrimp
Other prey	Anomura, bird, Bivalvia, Brachyura, Cancridea, Cephalopodia, Chaetognatha, *Chionoecetes bairdi*, *Chionoecetes opilio*, *Chionoecetes* spp., Cnidaria, crab, Crustcea, Ctenophora, Cumacea, Decapoda, Echinodermata, egg, fish egg, Gastropoda, Holothuroidea, invertebrate, Isopoda, Larvacea, Lithodidae, Majidae, Mollusca, Octopoda, Ophiuroidea, Paguridae, *Paralithodes platypus*, Polychaeta, Pteropoda, Teuthida, Tunicata, worm

Exploratory analysis confirmed that parameter estimates and the predictions of the spatio-temporal model are qualitatively similar when the number of knots is increased.

We also utilized the 20 km × 20 km spatial grid for the EBS to produce maps. This spatial grid covers a surface area of 495,827 km². The values of all spatial and spatio-temporal variation terms in each cell of the spatial grid for the EBS were equal to their values at the closest knot of the cell under consideration. Thus, the surface area associated with a given knot was estimated as the number of cells of the spatial grid for the EBS associated with the knot under consideration multiplied by the surface areas of these cells. Consequently, PESC for the different prey items was estimated in each year by replacing locations (i.e. the cells of the spatial grid for the EBS) by knots in Equation (6).

The standardized EBS bottom trawl surveys conducted by the AFSC also collect bottom temperature data (Figure S2). We did not integrate bottom temperature effects on predator biomass catch rate or prey-biomass-per-predator-biomass in our spatio-temporal model. However, we employed the bottom temperature data collected during the standardized EBS bottom trawl surveys to produce bottom temperature maps for each year of the period 1992–2015. We then used the bottom temperature maps to interpret the spatial patterns of PESCs predicted by our spatio-temporal model in each year of the period 1992–2015 in the light of the annual spatial patterns of bottom temperature in the EBS region.

2.4 | Data-limited case-study

Next, we carry out a second demonstration, in a data-limited situation, that is a more common situation when working with fish diet data. Specifically, we apply our spatio-temporal modelling approach for the red grouper population of the West Florida Shelf, a region located in the U.S. Gulf of Mexico (Figure 2a). The West Florida Shelf is a region characterized by very high biodiversity that is also under many anthropogenic and environmental pressures. This region is, therefore, the focus of substantial resource management efforts (Grüss, Rose, et al., 2017; O'Farrell, Grüss, Sagarese, Babcock, & Rose, 2017). However, despite this and the fact that numerous monitoring programmes sample fish populations on the West Florida Shelf, only a few regional fisheries-independent surveys have recently collected stomachs from large fish predators, including red grouper (Grüss, Perryman, et al., 2018). In addition, many of the stomachs from large fish predators that are collected on the West Florida Shelf are everted, as they are typically caught and brought up from deep waters (e.g. Bradley & Bryan, 1975; McCawley, Cowan, & Shipp, 2006). Thus, currently only a limited number of stomachs are available to understand the diet patterns of the red grouper population of the West Florida Shelf.

For the second demonstration, we rely on red grouper biomass catch rate and stomach content data that were collected by the SEAMAP (Southeast Area Monitoring and Assessment Program) groundfish trawl survey between 2011 and 2015 (Rester, 2017). The
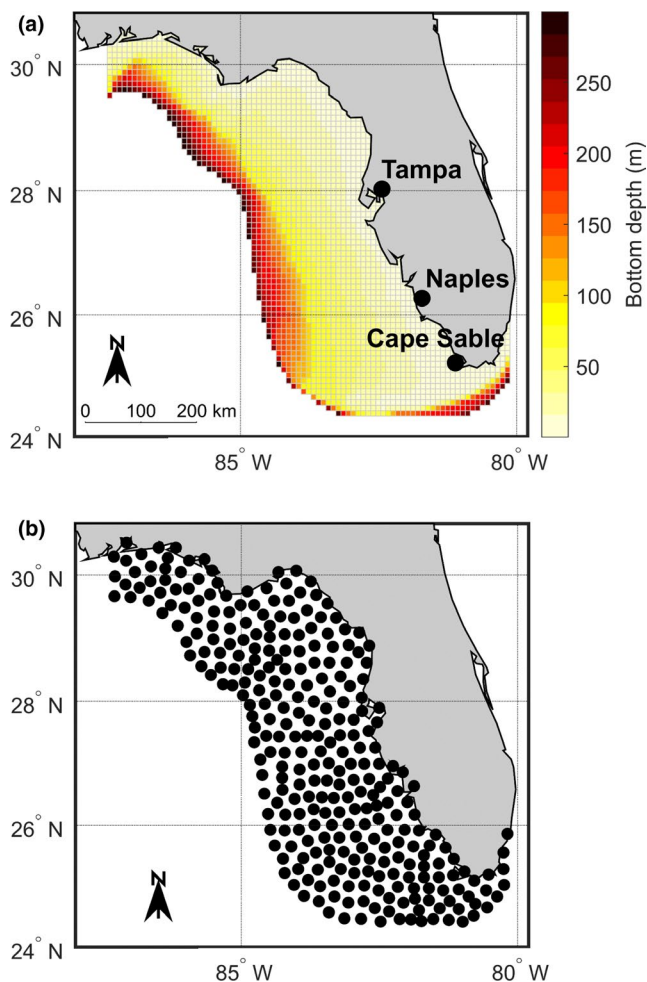
FIGURE 2 (a) Map of the West Florida Shelf in the Gulf of Mexico, showing bottom depth (in m) in the cells of the spatial prediction grid used for this region. (b) Spatial distribution of the "knots" specified to approximate all spatial and spatio-temporal variation terms for the West Florida Shelf

red grouper biomass catch rate data were obtained from SEAMAP (2019). The SEAMAP groundfish trawl survey collects biomass catch rate data over the entire U.S. Gulf of Mexico using a random sampling design, yet it opportunistically collects fish stomachs only in the West Florida Shelf region (Grüss, Perryman, et al., 2018; Appendix S2). In the U.S. Gulf of Mexico, red grouper is encountered quasi-exclusively on the West Florida Shelf (Grüss, Thorson, et al., 2017).

The prey items found in the red grouper stomachs collected by the SEAMAP groundfish trawl survey are rarely identified to the species, genus or family levels. Therefore, we considered four broad prey items for our demonstration for West Florida Shelf red grouper: crabs, fish, shrimps and a fourth item that aggregates all other prey found in red grouper stomachs which is referred to as "other prey" (Table 2). The original dataset, which was provided by the Fish and Wildlife Conservation Commission (FWC)'s Fisheries-Independent Monitoring Program (FIM), had 566 prey entries associated with a biomass value (in g) for the period 2011–2015, for a total of 269 red grouper stomachs collected in 121 hauls. We reorganized the

Prey item	Components
Crabs	*Acanthilia intermedia*, Brachyura, Calappidae, crab, *Damithrax hispidus*, *Euryplax nitida*, Goneplacidae, *Iliacantha* spp., Leucosiidae, *Lithadia* spp. *Macrocoeloma camptocerum*, *Macrocoeloma* spp., Majidae, Majoidea, *Microphrys bicornutus*, *Mithrax forceps*, *Mithrax pleuracanthus*, *Mithrax* spp., *Panopeus occidentalis*, Parthenopidae, *Pilumnus sayi*, *Pitho* spp., *Podochela riisei*, Portunidae, *Portunus* spp., *Stenorhynchus seticornis*, Xanthidae, Xanthoidea
Fish	Actinopterygii, Anguilliformes, Apogonidae, *Haemulon aurolineatum*, *Halichoeres bivittatus*, Monacanthidae, Muraenidae, *Trachurus lathami*
Shrimps	Alpheidae, Alpheoidea, *Alpheus* spp., Caridea, Dendrobranchiata, *Farfantepenaeus aztecus*, *Metapenaeopsis* spp., Palaemonidae, Penaeidae, Penaeoidea, *Periclimenes* spp., *Processa* spp., shrimp, *Sicyonia* spp., *Sicyonia typica*, Sicyoniidae, *Synalpheus* spp.
Other prey	Algae, Amphipoda, Annelida, Ascidiacea, Bivalvia, Crustacea, Decapoda, Dendrobranchiata, *Excorallana antillensis*, Galatheidae, Holothuroidea, Hydrozoa, Idoteidae, *Gonodactylus* spp., Loliginidae, macroalgae, *Meiosquilla schmitti*, Mollusca, *Munida pusilla*, *Neogonodactylus* spp., Ostracoda, Paguridae, *Petrolisthes galathinus*, Polychaeta, Porifera, Scyllaridae, *Scyllarus chacei*, *Squilla* spp., Squilloidea, Stomatopoda, Teuthida, Thalassinidea, *Upogebia* spp.

dataset around the four broad prey items (crabs, fish, shrimps and other prey), which then included 233 entries for the 148 red grouper stomachs collected in 79 hauls (Appendix S2). After averaging the biomass of each prey category in each haul (first step of our spatio-temporal modelling approach), the number of entries in the dataset reduced to 160. At this stage, some hauls had no entry for some of the prey items, and we treated these instances as an observation of zero biomass for those prey items in those hauls, resulting in a final dataset with a total of 79 × 4 = 316 entries (Figure S3). To obtain prey-biomass-per-predator-biomass data (in g per g of predator), we employed the red grouper length information provided along with prey biomasses in the dataset that the FWC's FIM shared with us. We transformed red grouper lengths expressed in cm standard length (SL) into lengths in cm total length (TL) using Christensen and Pauly's (1993) equation, and we then converted red grouper lengths expressed in cm TL into weights in g using the length–weight equation from SEDAR (2009).

As in the first case-study, we employed 300 knots uniformly distributed over a spatial grid to approximate all spatial and spatio-temporal variation terms (Figure 2b). Here as well, we chose a total of 300 knots, as this number of knots offered a good compromise between accuracy and computational speed, and exploratory analysis confirmed that parameter estimates and spatio-temporal model predictions are qualitatively similar when increasing the number of knots. We created a 0.09° (i.e. 10 km × 10 km) spatial grid for the West Florida Shelf for this study (Figure 2a). This spatial grid covers a surface area of 209,040 km². The bottom depth in the cells of this spatial grid ranges between 0 and 300 m, which is the depth range at which red grouper is found on the West Florida Shelf (Grüss, Thorson, et al., 2017). The bottom depth in each cell of the spatial grid was determined from a raster of bottom depth with a resolution of 0.09°, which was constructed from the 15 arc-second (~500 m) resolution bathymetry grid predicted by the Coastal Relief

Model for the Gulf of Mexico that is available via the Gulf of Mexico Coastal Observing System (GCOOS, 2018). Based on preliminary tests, we ignored geotropic anisotropy (i.e. assumed isotropy) in the calculation of the spatial correlation among locations (i.e. the **R** terms in Equation 5) to ensure the convergence of the spatio-temporal model.

2.5 | Comparisons with other approaches to estimating diet proportions

In the two case-studies, we also compared the diet proportions predicted by our spatio-temporal model to the diet proportions predicted by: (a) a non-spatial version of our model (hereafter referred to as the "non-spatial model"), that is a version of our model where spatial and spatio-temporal variation are ignored; (b) the simple average method applied to prey biomass data; and (c) the Ainsworth method applied to prey biomass data. Our intention was to determine whether differences in predictions were due to the spatial component of our analysis (comparing the estimates of the spatial and non-spatial models), or whether they were due to the model formulation itself (comparing non-spatial model estimates to the estimates generated by the simple average and Ainsworth methods). In the data-rich case-study, we estimated diet proportion estimates, as well as associated standard errors (except for the simple average method), for each year of the period 1992–2015. On the other hand, in the data-limited case-study, it was not possible to generate estimates for individual years with the Ainsworth method. The Ainsworth method requires a minimum of 30 data points for each individual year (Morzaria-Luna et al., 2018). Therefore, in the data-limited case-study, we estimated diet proportions, as well as associated standard errors (except for the simple average method), for the entire period 2011–2015.

3 | RESULTS

3.1 | Data-rich case-study

All the prey-biomass-per-predator-biomass and predator biomass catch rate data for the data-rich case-study were collected in June–September. Therefore, the diet patterns reported in the data-rich case-study represent summertime patterns. As the EBS is a marine region characterized by strongly contrasting seasons, EBS large walleye pollock diet patterns vary greatly from one season to another (Dwyer, Bailey, & Livingston, 1987; Livingston, Ward, Lang, & Yang, 1993). The walleye pollock individuals considered in this study measured between 55 and 89 cm TL; 52% of them belonged to the 55–62 cm length category and the other 48% belonged to the 63+ cm length category (Figure S4).

The spatio-temporal model predicted that, over the period 1992–2015, Euphausiacea usually had the largest contribution by weight to large walleye pollock diet, followed by fish and shrimps (Figure 3a). Notably, the proportion of fish in large walleye pollock diet decreased substantially over the period 1992–2008 and then increased markedly between 2009 and 2015. In 2015, the proportion

of fish in large walleye pollock diet (0.41) was greater than that of Euphausiacea (0.27). Amphipods made up a low proportion of large walleye pollock diet over the period 1992–2001. Then, in the period 2002–2015, the proportion of amphipods in large walleye pollock diet was highly variable, oscillating between low and relatively high values and sometimes exceeding the proportion of shrimps and/ or fish in large walleye pollock diet (e.g. in 2010, where amphipod biomass made up 31% of large walleye pollock diet, while the proportions of shrimps and fish in large walleye pollock diet were 0.08 and 0.16, respectively). Finally, copepods, Mysidacea and other prey tended to have similar low proportions in large walleye pollock diet (Figure 3a).

The input sample size, which was estimated from diet proportions and their variance, tended to decrease between 1992 and 2005 and to increase afterwards (Figure 3b). The input sample size was highest between 1992 and 2000. It was often greater than the number of locations where large walleye pollock stomachs were collected, except between 2003 and 2012 where the input sample size and the number of locations sampled were similar (Figure 3b).

The spatio-temporal model predicted that, over the period 1992–2015, total PESC (i.e. PESC for all prey items combined)
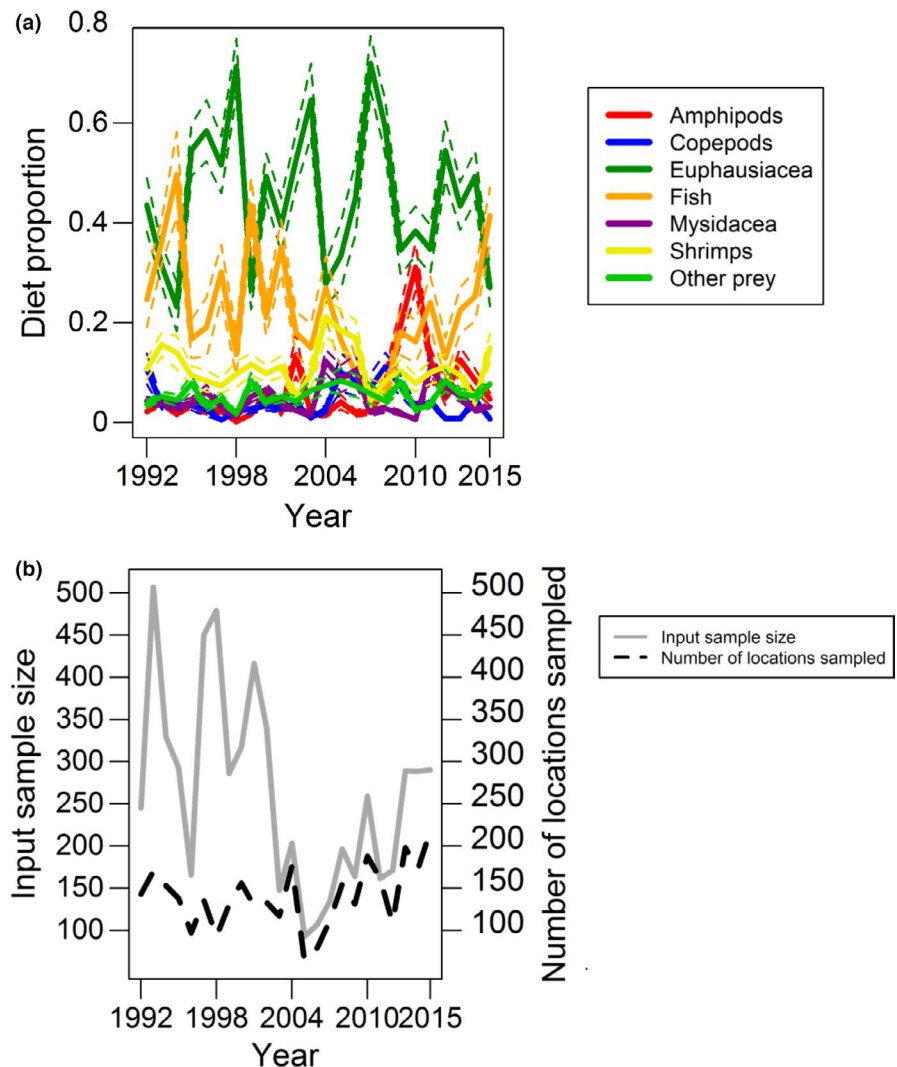
FIGURE 3 (a) Proportions of amphipods, copepods, Euphausiacea, fish, Mysidacea, shrimps and other prey in the diet of large (55+ cm) eastern Bering Sea walleye pollock (*Gadus chalcogrammus*, Gadidae) over the period 1992–2015 predicted by the spatio-temporal model (solid lines: predicted value; dashed lines: ±1 *SE*). (b) Number of locations sampled in each year of the period 1992–2015, and input sample size in each of these years predicted by the spatio-temporal model

exhibited a large decline; the bulk of this decline took place between
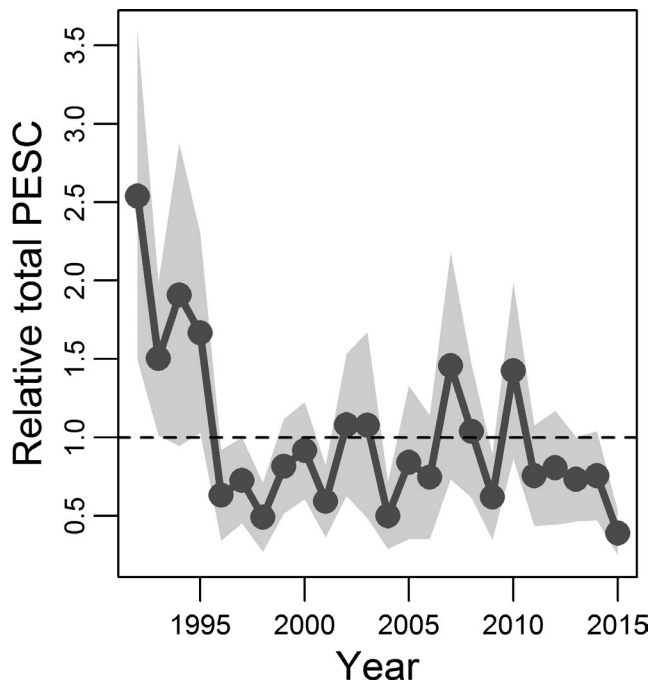
FIGURE 4 Trends in total predator-expanded-stomach-contents (PESC) over the period 1992–2015 predicted by the spatio-temporal model developed for large (55+ cm) eastern Bering Sea walleye pollock (*Gadus chalcogrammus*, Gadidae; solid lines: predicted value; shaded area: 95% confidence interval). To produce this figure, model predictions for individual years were divided by mean model predictions over the period 1992–2015

1992 and 1995 (Figure 4). The decline in total PESC mirrored the overall decrease in PESC for all individual prey items except amphipods between 1992 and 2015 (Figure S5). The PESC for amphipods was relatively constant, except for 2010 where it was anomalously high (Figure S5). The patterns of change in large walleye pollock biomass over the period 1992–2015 were different from the patterns of change in total PESC (Figure S6). Specifically, the biomass of large walleye pollock showed a pronounced decrease between 1992 and 1998, a pronounced increase between 1998 and 2003, and then no marked trend between 2003 and 2015.

On average over the period 1992–2015, the spatial patterns of PESC varied largely from one prey item to another (Figure 5). PESC for amphipods was highest in the northern and central parts of the Middle Shelf of the EBS, particularly around St. Matthew Island (Figure 5a). PESC for copepods was highest in the central and southern parts of the Middle and Outer Shelves of the EBS, especially along the Alaska Peninsula and around the Pribilof Islands (Figure 5b). The highest PESCs for Euphausiacea occurred along the Alaska Peninsula (Figure 5c), while those for fish occurred in the northern and central parts of the Outer Shelf of the EBS (Figure 5d). PESC for Mysidacea was greatest in the central and southern parts of the Inner and Middle Shelves of the EBS (Figure 5e). Hotspots of PESC for shrimps were found in the northern part of the Middle and Outer Shelves of the EBS (Figure 5f). Finally, PESC for other prey was constant over space (Figure 5g).

The spatial patterns of PESCs also varied somewhat between individual years of the period 1992–2015 (Figures 6 and 7; Figure S7). Notably, if we consider bottom temperatures in the EBS region, the
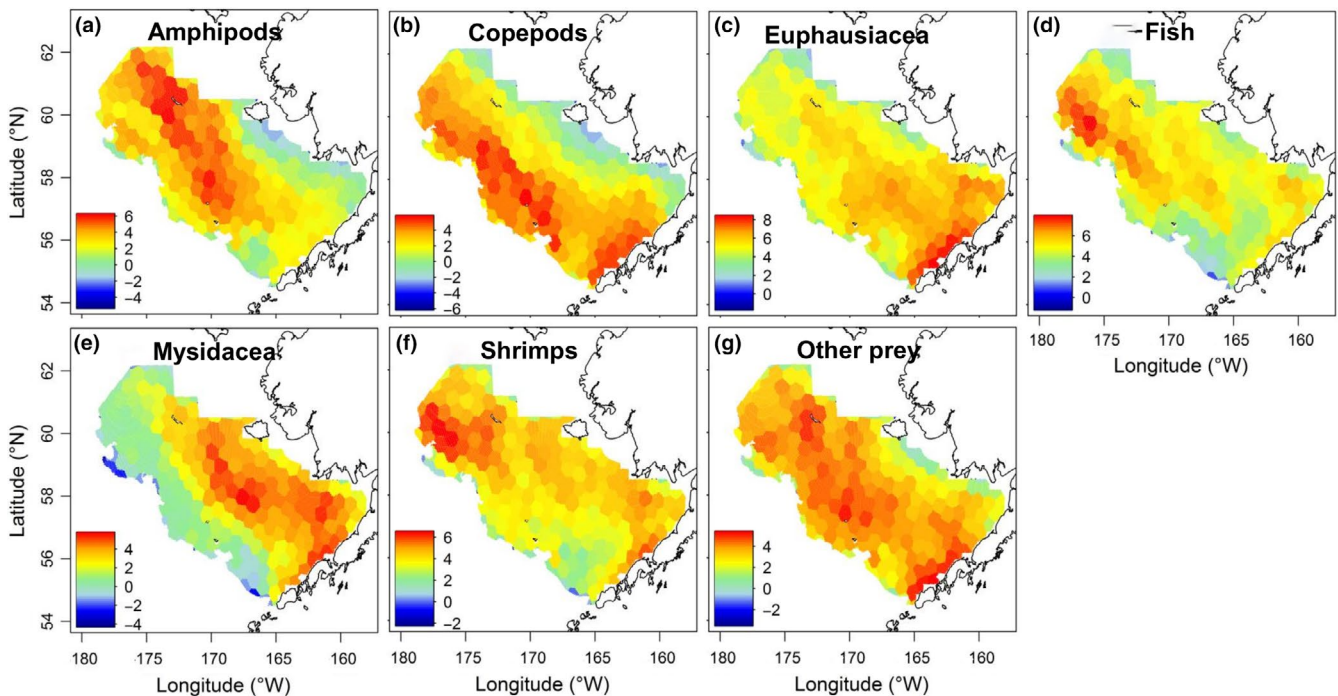
FIGURE 5 Mean log-predator-expanded-stomach-contents over the period 1992–2015 predicted by the spatio-temporal model developed for large (55+ cm) eastern Bering Sea walleye pollock (*Gadus chalcogrammus*, Gadidae). The colour legends are provided in the top rows and have units ln(tons)

spatial patterns of PESCs differed largely between very cold (e.g. 1999 or 2012) and very warm (e.g. 2003 or 2015) years (Figures 6 and 7; Figure S7). Thus, PESC for copepods was high on the Middle Shelf of the EBS and very low on the Inner Shelf in 1999 and 2012 (very cold years), while hotspots of PESC for copepod occurred on the Outer Shelf, around St. Matthew Island and along the Alaska Peninsula in 2003 and 2015 (very warm years; Figures 6 and 7). Hotspots of PESC for Euphausiacea were found throughout the Inner and Middle Shelves of the EBS in 1999 and 2012 (very cold years), whereas they concentrated on the Middle Shelf and along the Alaska Peninsula in 2003 and 2015 (very warm years). Finally, PESC for fish was greatest throughout the Middle and Outer Shelves of the EBS in 1999 and 2012 (very cold years), while the highest values of PESC for fish occurred in the northern part of the Middle and Outer Shelves in 2003 and 2015 (very warm years). However, in 2015 (the warmest year of the period 1992–2015), PESC for fish was also high on the Inner Shelf of the EBS (Figure 7).

3.2 | Data-limited case-study

The red grouper stomachs used in the present study were collected between June and October. However, the West Florida Shelf is not characterized by strongly contrasting seasons, and red grouper is a resident species that does not undertake seasonal migrations and is reported to feed primarily on benthic invertebrates (Coleman et al., 2010). Therefore, it is reasonable to assume that the diet patterns

of red grouper between June and October are reflective of the diet patterns of the species in the other months of the year. Most of the red grouper stomachs available to us were from individuals measuring between 15 and 34.1 cm TL (Figure S8), that is older juvenile red groupers (Fitzhugh, Lyon, Walling, Levins, & Lombardi-Carlson, 2006; Lombardi-Carlson et al., 2008).

The spatio-temporal model predicted that crabs had the largest contribution by weight to red grouper diet in all years of the period 2011–2015, except in 2012 where "other prey" (i.e. prey other than crabs, fish or shrimps) had the largest contribution by weight to red grouper diet (Figure 8a). The proportion of other prey in red grouper diet was greater than those of fish and shrimps in 2011 and 2012, and then lower than those of fish and shrimps between 2013 and 2015. Fish and shrimps had similar low proportions in red grouper diets over the entire study period (Figure 8a).

The input sample size estimated from diet proportions and their variance was noticeably large in 2014 (Figure 8b), a year where the proportion of crabs in red grouper diet was at its highest, while the proportions of shrimps and other prey were at their lowest (Figure 8a). The input sample size was greater than the number of locations where red grouper stomachs were collected in all years of the study period (Figure 8b).

The spatio-temporal model predicted that total PESC was constant over the period 2011–2015 (Figure 9). PESC for crabs and shrimps was relatively constant between 2011 and 2015 (Figure S9). By contrast, between 2011 and 2015, PESC for fish increased greatly, while PESC for other prey declined markedly (Figure S9). In
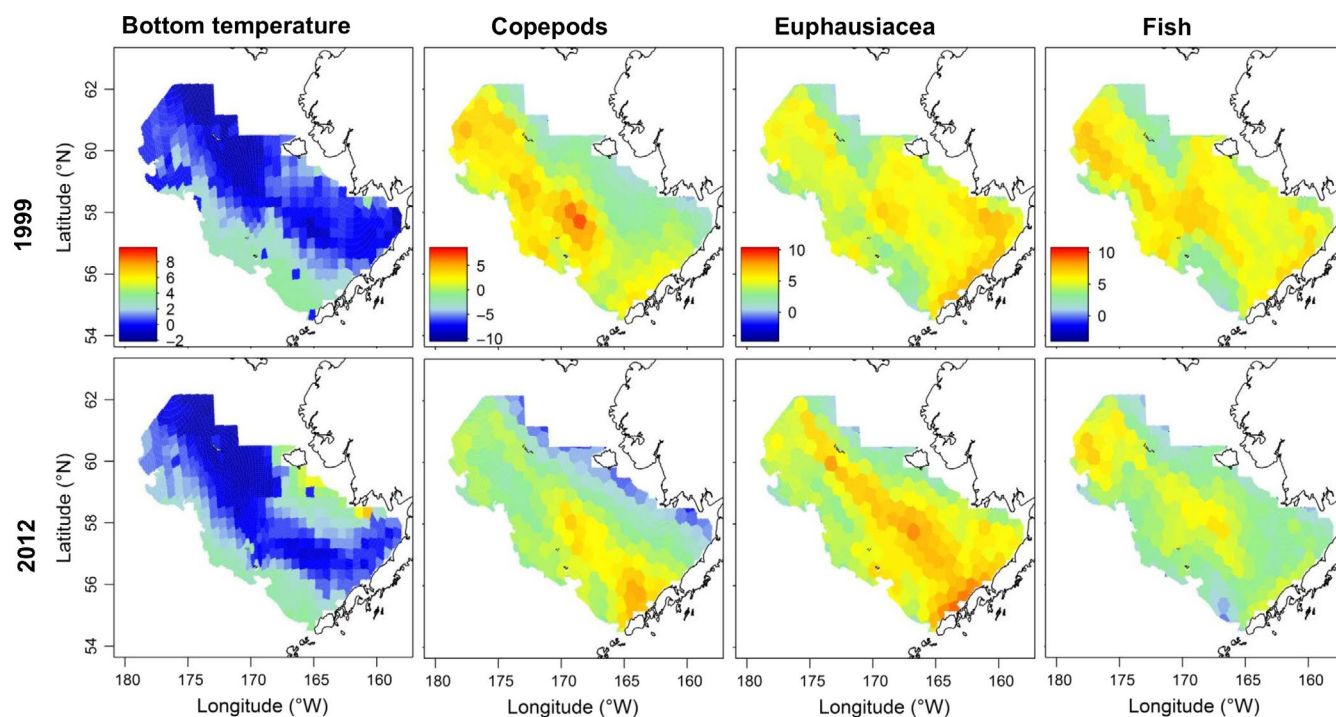
FIGURE 6 Bottom temperature and log-predator-expanded-stomach-contents predicted by the spatio-temporal model developed for large (55+ cm) eastern Bering Sea walleye pollock (*Gadus chalcogrammus*, Gadidae), in the very cold years of 1999 and 2012. The colour legends are provided in the top rows and have units °C in the case of bottom temperatures, and ln(tons) in the case of log-predator-expanded-stomach-contents
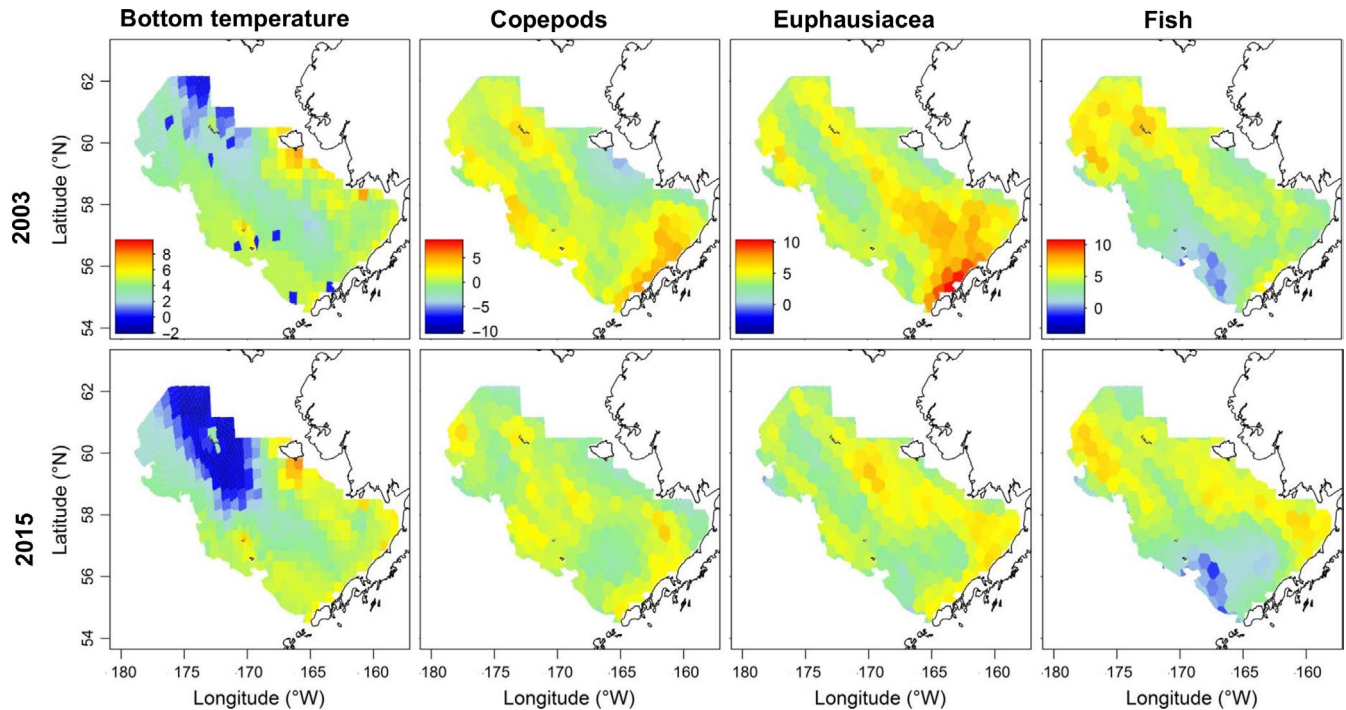
FIGURE 7 Bottom temperature and log-predator-expanded-stomach-contents predicted by the spatio-temporal model developed for large (55+ cm) eastern Bering Sea walleye pollock (*Gadus chalcogrammus*, Gadidae), in the very warm years of 2003 and 2015. The colour legends are provided in the top rows and have units °C in the case of bottom temperatures, and ln(tons) in the case of log-predator-expanded-stomach-contents
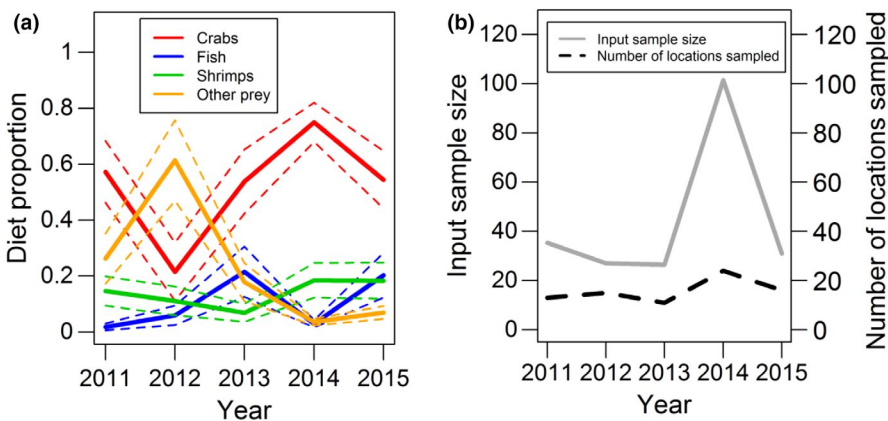
FIGURE 8 (a) Proportions of crabs, fish, shrimps and other prey in the diet of West Florida Shelf red grouper (*Epinephelus morio*, Epinephelidae) over the period 2011–2015 predicted by the spatio-temporal model (solid lines: predicted value; dashed lines: ±1 *SE*). (b) Number of locations sampled in each year of the period 2011–2015, and input sample size in each of these years predicted by the spatio-temporal model

parallel, the spatio-temporal model predicted that red grouper bio-mass decreased largely between 2011 and 2015 (Figure S10).

On average over the period 2011–2015, the spatial patterns of PESC for individual prey items were relatively similar (Figure 10). Hotspots of PESC for crabs, fish, shrimps and other prey occurred in the region of south-western Florida between Naples and Cape Sable. Another area where PESC for shrimps and other prey was high was the region north-west of Tampa (Figure 10).

The spatial patterns of PESCs were relatively similar from one year of the study period to the next (Figure 11; Figure S11). However, the year 2012 was characterized by higher PESC for all prey items in the region north-west of Tampa, while the year 2014 was charac-terized by lower PESC for all prey items in the region north of 28°N

(Figure 11). The spatial patterns of PESCs in 2012 and 2014 mir-rored the spatial patterns of red grouper biomass in those 2 years (Figure S12).

3.3 | Comparisons with other approaches to estimating diet proportions

Our spatio-temporal model, the non-spatial version of our model and the Ainsworth and simple average methods generally predicted similar diet proportions (Appendix S3). However, the diet propor-tions predicted by the non-spatial model tended to be more similar to those predicted by the spatio-temporal model compared to the
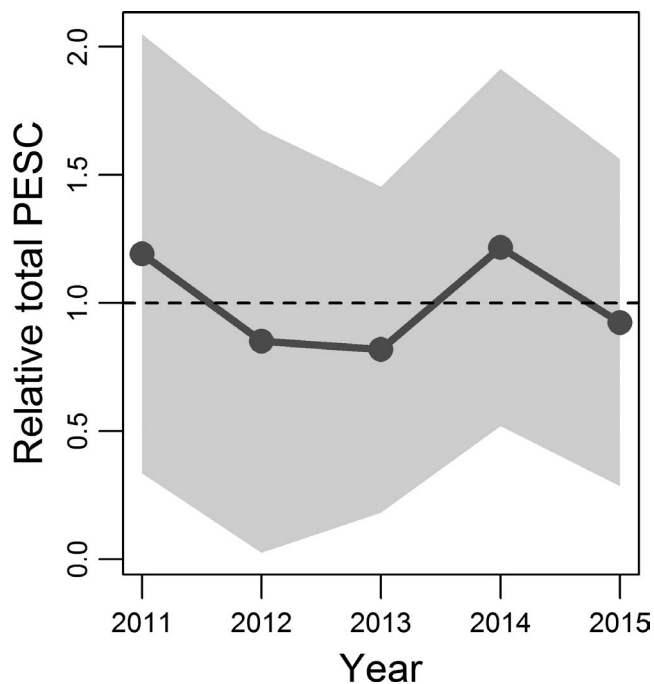
FIGURE 9 Trends in total predator-expanded-stomach-contents (PESC) over the period 2011–2015 predicted by the spatio-temporal model developed for West Florida Shelf red grouper (*Epinephelus morio*, Epinephelidae; solid lines: predicted value; shaded area: 95% confidence interval). To produce this figure, model predictions for individual years were divided by mean model predictions over the period 2011–2015

Ainsworth and simple average methods. In the data-rich case-study, the standard errors associated with diet proportions estimated by the Ainsworth method were, in general, greater than those predicted by the spatio-temporal and non-spatial models. In the data-limited case-study, the standard errors associated with diet proportions estimated by the non-spatial model were larger than those predicted by the spatio-temporal model and the Ainsworth method (Appendix S3).

4 | DISCUSSION

We developed a novel approach that allows for spatio-temporal analyses of diet data, which we applied in a data-rich situation (EBS large walleye pollock) and in a more common, data-limited situation (West Florida Shelf red grouper). Our approach fits a spatio-temporal statistical model to both prey-biomass-per-predator-biomass data and predator biomass catch rate data to reveal spatial and temporal patterns in the relative biomasses of prey eaten immediately prior to sampling by the predator of interest (predator-expanded-stomach-contents or PESCs). By accounting for fine-scale spatio-temporal structure while expanding individual stomach samples to population-level estimates of predation, our novel approach reveals important fine-scale diet patterns and avoids biases in estimating predation pressure at the population level. In this way, our approach represents a substantial

improvement on traditional, non-spatial approaches to estimating diet compositions and consumption.

We found that our spatio-temporal modelling approach predicts diet proportions that are relatively similar to those predicted by other approaches (the simple average and Ainsworth methods), but have generally similar or better precision, which is particularly valuable if our approach is to be used for supporting resource management. For the sake of demonstration, our applications considered a limited number of prey items (seven in the data-rich situation and four in the data-limited situation). However, with R package VAST, it will be possible for future studies employing our approach to fit spatio-temporal models that consider a much larger number of prey items (Thorson & Haltuch, 2018), although the issue of computation time will need to be addressed (see below). Considering all potential prey of the predators of interest will be especially important if the aim of future studies applying our approach is to inform the parameterization of "whole ecosystem models" such as Ecopath with Ecosim models (Christensen & Walters, 2004; Pauly, Christensen, & Walters, 2000) and Atlantis models (Fulton et al., 2004, 2011). In these ecosystem models, new predator–prey linkages are not initiated at run time. Therefore, when estimating diet proportions for parameterizing these ecosystem models, it is necessary to consider all the potential prey items of the predators that these models represent (Ainsworth et al., 2010). In addition to whole ecosystem models, other fisheries research tools and investigations will benefit from our spatio-temporal modelling approach, as discussed below.

Our data-rich case-study supports findings from previous studies and provides new insights into the diet patterns of large walleye pollock in the EBS during summer. Although EBS large walleye pollock can consume a diversity of prey organisms (Table 1), only Euphausiacea, fish, shrimps and, to a lesser extent, amphipods usually make up the bulk of their food (Figure 3a; Buckley et al., 2016; Dwyer et al., 1987; Livingston et al., 2017). Similar to Boldt, Buckley, Rooper, and Aydin (2012), we found that the contribution of fish biomass to large walleye pollock diet decreased markedly until the late 2000s. Our spatio-temporal model also predicted a large increase in the proportion of fish in large walleye pollock diet between 2009 and 2015, which resulted in fish becoming the dominant prey by weight in large walleye pollock diet in 2015. The predictions of our spatio-temporal model also concurred with Buckley et al. (2016) in that the contribution of amphipod biomass to large walleye pollock diet became highly variable in the early 2000s, oscillating between low and relatively high values over the recent period. Our results for fish and amphipod prey may be in large part due to the important changes in bottom temperatures that have occurred in the EBS region since the early 2000s. Overall, the period 2002–2015 was characterized by a succession of very warm and very cold years (Figure S2; Buckley et al., 2016; Eisner, Napp, Mier, Pinchuk, & Andrews, 2014). Very warm years are associated with low amphipod biomass and low amphipod consumption by walleye pollock, while very cold years (e.g. 2010) are characterized by high amphipod biomass and an anomalously high proportion of amphipods in large walleye pollock diet (Buckley et al., 2016). Moreover, in warm years, a reduction in
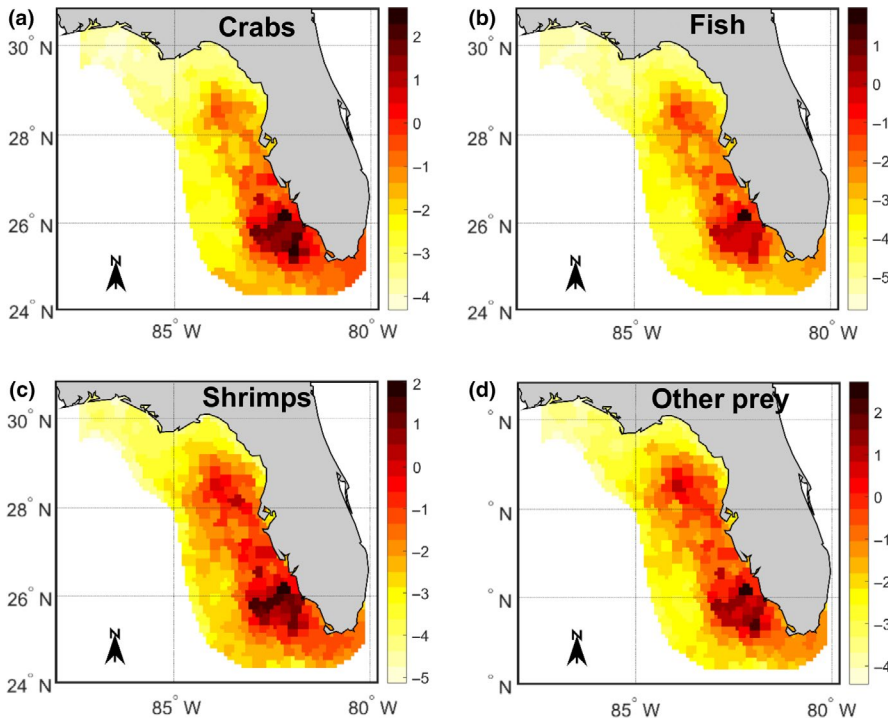
FIGURE 10 Mean log-predator-expanded-stomach-contents over the period 2011–2015 predicted by the spatio-temporal model developed for West Florida Shelf red grouper (*Epinephelus morio*, Epinephelidae). The colour legends are provided in the top rows and have units ln(tons)
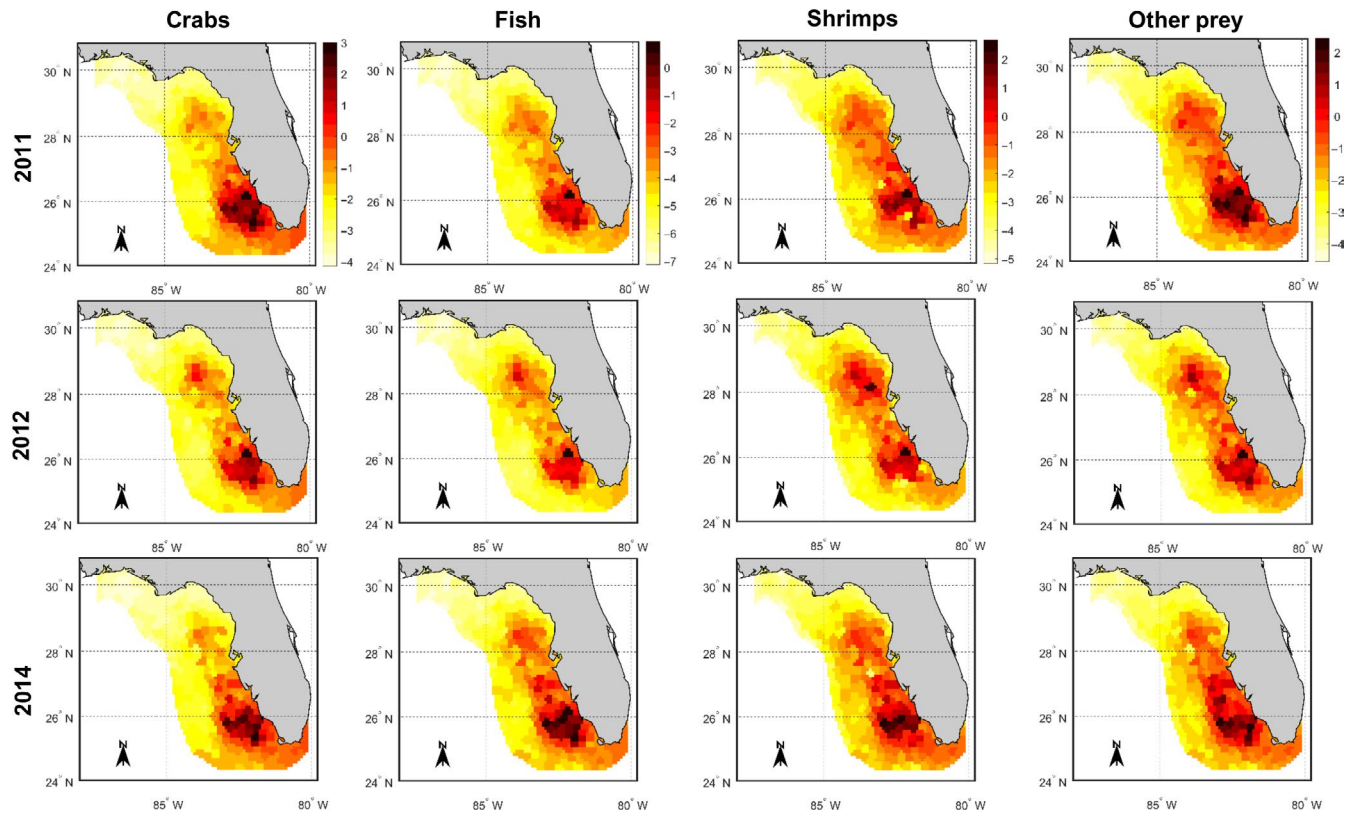
FIGURE 11 Log-predator-expanded-stomach-contents predicted by the spatio-temporal model developed for West Florida Shelf red grouper (*Epinephelus morio*, Epinephelidae), for the years 2011, 2012 and 2014. The colour legends are provided in the top rows and have units ln(tons)

the extent of the cold pool (i.e. the area of the EBS with bottom temperatures at or below 2°C) is accompanied by an expansion of the area occupied by walleye pollock, which allows this species to access the Middle Shelf where the cold pool would usually restrict its occurrence, and where fish prey are abundant (Hunt, Stabeno, Strom, & Napp, 2008; Kotwicki, Buckley, Honkalehto, & Walters,

2005). Boldt et al. (2012) found that small walleye pollock makes up a great fraction of the fishes consumed by EBS walleye pollock, and that the amount of cannibalism of walleye pollock increased when bottom temperatures increased in the EBS region. Moreover, EBS walleye pollock spawning stock biomass (SSB) greatly increased over the period 2009–2015 according to stock assessments (Ianelli et al., 2018). Therefore, we conclude that the increase in the proportion of fish in large walleye pollock diet between 2009 and 2015 (except for 2012) may be mainly explained by both the marked increase in bottom temperature and the large increase in walleye pollock SSB that occurred in the EBS region between 2009 and 2015.

The mean spatial patterns of PESCs over the period 1992–2015 predicted by our spatio-temporal model concur with the spatial patterns of consumptions by large walleye pollock reported in previous studies (Boldt et al., 2012; Buckley et al., 2016; Dwyer et al., 1987; Livingston et al., 2017). With respect to the dominant prey by weight in the diet of large walleye pollock, our study, Buckley et al. (2016) and Livingston et al. (2017) found that: (a) the relative biomass of Euphausiacea eaten by large walleye pollock is more important in the south-eastern than in the north-western part of the EBS, (b) the relative biomass of fish eaten by large walleye pollock is greatest in the northern and central parts of the Outer Shelf of the EBS, and (c) the bulk of the relative biomass of shrimps eaten by large walleye pollock occurs in the northern part of the Middle and Outer Shelves of the EBS. As mentioned earlier, small walleye pollock makes up a great proportion of the fish eaten by large walleye pollock (Boldt et al., 2012; Dwyer et al., 1987; Livingston et al., 2017). Predation of small walleye pollock by arrowtooth flounder (*Atherestes stomias*, Pleuronectidae) and, to a lesser extent, Pacific cod (*Gadus macrocephalus*, Gadidae) and Pacific halibut (*Hippoglossus stenolepis*, Pleuronectidae) is also considerable (Livingston et al., 2017). Given the large predation pressure exerted on small walleye pollock and the high economic importance of EBS walleye pollock (Aydin & Mueter, 2007), we recommend that future studies employ our spatio-temporal modelling approach to specifically explore the spatial and temporal patterns of predation on small walleye pollock, so as to better inform EBFM in the EBS region.

The spatial patterns of PESCs predicted by our spatio-temporal model in the large walleye pollock case-study differ greatly between prey items, but also between years. Notably, PESCs were predicted to be higher on the Middle Shelf of the EBS in the very warm years of 2003 and 2015. For example, in the very warm years of 2003 and 2015, the highest values of PESC for Euphausiacea were found on the Middle Shelf of the EBS and along the Alaska Peninsula, while the highest values of PESC for fish occurred in the northern part of the Middle and Outer Shelves. These results may stem from the reduction of the extent of the cold pool and the resulting expansion of the area occupied by walleye pollock on the Middle Shelf of the EBS in warm years, which we already mentioned earlier. This increase in the area occupied by walleye pollock may offer better foraging opportunities to walleye pollock and, in particular, more access to fish prey (Boldt et al., 2012; Hunt et al., 2008; Kotwicki et al., 2005), and it may ultimately lead to a considerable improvement in walleye

pollock condition (Boldt, Rooper, & Hoff, 2015; Grüss et al., 2020; Siddon & Zador, 2018).

Our data-limited case-study relied mainly on diet data for the older juvenile red grouper life stage and very likely provides insights into the spatio-temporal diet patterns of this life stage during all seasons of the year. We found that crabs had the largest contribution by weight to West Florida Shelf red grouper diet, except in 2012 where prey other than crabs, fish and shrimps made up the largest proportion of red grouper diet. This result is consistent with the diet proportions that Masi et al. (2014) estimated for red grouper using the Ainsworth method for parameterizing the diet matrix of the Atlantis model of the Gulf of Mexico (crabs and lobsters: 44.45%; small reef fish: 31.35%; "other shrimps": 24.20%). Our spatio-temporal model also predicted that red grouper total PESC was constant between 2011 and 2015, while red grouper biomass decreased markedly over the same time period, consistent with Thompson et al. (2018). The absence of a decline in red grouper total PESC during a decrease in red grouper biomass may reflect a release in competition within the red grouper population of the West Florida Shelf.

The spatial patterns of PESCs predicted in the red grouper case-study are similar to the spatial distribution patterns of older juvenile red grouper estimated using spatio-temporal binomial models (Grüss, Perryman, et al., 2018; Grüss, Thorson, Babcock, & Tarnecki, 2018; Grüss, Thorson, et al., 2017). Older juvenile red grouper was found to have a higher probability of encounter in south-western Florida (south of 28°N) than in north-western Florida (north of 28°N), potentially due to differences in habitat availability and higher mortality rates in north-western Florida caused by red tides, a type of harmful algal bloom (Grüss, Thorson, et al., 2017; Lombardi-Carlson et al., 2008). Thus, the larger PESCs in the region north-west of Tampa in 2012 (or lower PESCs in 2014) may be due to the fact that red tide severity was low in 2012 (and high in 2014) compared to other years of the 2010s (Sagarese et al., 2018).

In both the data-rich and data-limited case-studies considered in this study, the diet proportions generated using our spatio-temporal modelling approach were generally at least as precise as the diet proportions generated using the Ainsworth method, and often more precise. Thus, we can conclude that predicting diet proportions from the PESCs estimated by a delta model fitted to prey-biomass-per-predator-biomass and predator biomass catch rate data rather than predicting diet proportions from a Dirichlet model fitted to prey biomass data can result in more precise predictions. By contrast, the data-rich and data-limited case-studies differed in that our spatio-temporal modelling approach yielded more precise diet proportion estimates than a non-spatial version of our approach in the data-limited situation, but not in the data-rich situation. Therefore, we conclude that accounting for spatial and spatio-temporal variation in the delta model fitted to prey-biomass-per-predator-biomass and predator biomass catch rate data can result in more precise diet proportion estimates in data-limited situations. In data-limited situations, accounting for correlation among locations and, therefore, unmeasured variation in predator biomass catch rate and diet composition, can provide a very large amount of information to

our statistical model, thereby substantially improving its precision (Grüss, Thorson, et al., 2017; Thorson et al., 2015).

One important limitation of our spatio-temporal modelling approach in its current configuration is computation time. For example, it took more than nine hours with a laptop with a 2.9 GHz Intel Core i7-4910MQ processor to run the spatio-temporal model for EBS large walleye pollock for the present study. One solution to this issue is to restrict the number of prey categories considered in the spatio-temporal model to a minimum if the research focuses on specific prey items (e.g. small walleye pollock). Otherwise, we recommend that future studies implement our spatio-temporal modelling framework on clusters of calculations. This will be the best option to facilitate the exceedingly long simulations that will be needed to estimate diet proportions for the large number of predators typically represented in whole ecosystem models such as Ecopath with Ecosim models (Christensen & Walters, 2004; Pauly et al., 2000) and Atlantis models (Fulton et al., 2004, 2011).

As mentioned earlier, one of the uses of the estimates generated by our spatio-temporal modelling approach will be the parameterization of the diet matrices fed into dynamic multispecies models (e.g. Livingston & Jurado-Molina, 2000; Kinzey & Punt, 2009; Holsman et al., 2016) and whole ecosystem modelling platforms (e.g. Ecopath with Ecosim. Pauly et al., 2000; Christensen & Walters, 2004; Atlantis; Fulton et al., 2004, 2011). Other ecosystem modelling platforms do not require a diet matrix, yet can also benefit from the diet proportion estimates generated by our spatio-temporal model. For example, the spatially explicit individual-based, multispecies OSMOSE modelling platform (Grüss et al., 2016; Shin & Cury, 2001) does not employ a diet matrix, but rather predicts diet compositions based on predator–prey spatial overlap (i.e. predator–prey overlap in the horizontal dimension), predator–prey size ratios and the accessibility of prey to predators (e.g. due to predator–prey overlap in the vertical dimension). The validation of OSMOSE models could include a comparison of the diet proportions predicted by OSMOSE models with the diet proportions estimated by our spatio-temporal model.

The PESCs predicted by our spatio-temporal modelling approach can also be used to support ecosystem modelling efforts in other ways. The trends in PESCs estimated by the spatio-temporal model could be employed, along with time series of abundance and fisheries catch data, to calibrate Ecosim and Atlantis parameters (particularly Ecosim vulnerability parameters; Christensen & Walters, 2004), provided that the diet matrix fed into Ecopath or Atlantis was constructed using independent diet data. Moreover, the spatial patterns of PESCs estimated by the spatio-temporal model could be employed to validate Ecospace models (i.e. the spatial extensions of Ecopath with Ecosim models; Walters, Christensen, Walters, & Rose, 2010; Walters, Pauly, & Christensen, 1999), provided that the Ecopath diet matrix was generated using independent diet data.

The predictions of our spatio-temporal modelling approach could also be utilized to assist many EBFM efforts other than ecosystem modelling. For instance, the diet proportions estimated by our approach could be used by other EBFM tools, including the PREP (Predator Response to the Exploitation of Prey) equation (Pikitch

et al., 2012) and the SURF (Supportive Role to Fishery ecosystems) index (Plagányi & Essington, 2014). The PREP equation is a statistical equivalent of the Ecosim predator response to declines in prey populations, which was developed for quantifying the potential effects of decreases in forage fish abundance on predator abundance (Pikitch et al., 2012). The SURF index employs diet proportions to determine food web connectivity and identify the species whose decline may have large ecosystem-level effects (Plagányi & Essington, 2014). Other potential uses of our approach to support EBFM might consist of employing the estimated landscapes of PESCs to identify critical feeding hotspots of vulnerable species so as to limit competition for forage fish between these vulnerable species and fisheries (Pikitch et al., 2012); and to locate areas where marine predators exploit fisheries discards, so as to more comprehensively understand the potential impacts of discard mitigation measures (Kelleher, 2005).

There are also many fundamental ecological questions that can be tackled using the PESCs predicted by our spatio-temporal model. One of the most pressing issues to address is the ability of spatial predator–prey overlap indices to adequately reflect the strength of predator–prey interactions. This important issue could be tackled by examining whether the metrics of spatial overlap between predator and prey distributions reviewed in a recent study (Carroll et al., 2019) adequately reflect the incidence and intensity of predation suggested by PESC estimates. By exploring the relationship between predator–prey spatial overlap metrics and PESC estimates, one will be able to better understand how climate-driven changes in spatial overlap between predators and their prey might influence predation pressure, thereby contributing to changes in ecosystem function (Carroll et al., 2019; Hunsicker et al., 2013; Selden et al., 2018). Our spatio-temporal modelling approach also offers the possibility to explore issues of emergent multiple predator effects on prey within landscapes and niche partitioning, by implementing statistical models fitted to data rather than relying on theoretical simulation models (Northfield, Barton, & Schmitz, 2017). We encourage future studies to employ a version of our spatio-temporal model focusing on specific prey items (e.g. juvenile walleye pollock) and fitted to biomass catch rate and stomach content data for multiple predators (e.g. arrowtooth flounder, Pacific cod, Pacific halibut and walleye pollock). The annual landscapes of PESC predicted by this version of our spatio-temporal would be informative about long-term multiple predator–prey spatial dynamics and the degree of niche partitioning between the major predators of the prey of interest. Such insights would greatly improve our understanding of ecosystem structure and would allow us to better predict the consequences of changing species distributions and population sizes under climate change (Carroll et al., 2019; Hunsicker et al., 2013; Selden et al., 2018).

The variances and input sample sizes estimated by our spatio-temporal model will also benefit ecosystem modelling studies and multispecies stock assessments. The variances associated with diet proportions (Equation 8) can be employed for sensitivity and uncertainty analyses to understand the behaviour and uncertainties of ecosystem models and, consequently, lend more confidence to the information provided by these models (Grüss, Rose, et al.,

2017; O'Farrell et al., 2017; Rose et al., 2015; Saltelli, Tarantola, Campolongo, & Ratto, 2004). For example, the estimated variances can be used to produce hundreds of alternative diet compositions for the predators of interest, to then evaluate the variability of ecosystem model predictions in relation to uncertainty in diet compositions (Koehn et al., 2016; Morzaria-Luna et al., 2018). The input sample sizes estimated by our spatio-temporal model (Equation 9) can be utilized as starting points or upper bounds in multispecies stock assessment models, and be subjected to down- or up-weighting when assessment models are built, based on the goodness of fit of diet compositions (estimated by our approach) to the assessment models (Thorson, 2014).

In this study, we focused on %W estimates, that is the average per cent weight of prey items in predators' stomachs. However, fish diet studies also frequently measure the average per cent number of prey categories in predators' stomachs (%N) and the per cent frequency of occurrence of prey categories in predators' stomachs (%FO; Brown, Bizzarro, Cailliet, & Ebert, 2012; Cortés, 1997; Hyslop, 1980; Liao et al., 2001). Employing prey count and prey occurrence data in addition to prey biomass data in spatio-temporal modelling studies would increase the sample size, reduce the occurrence of model non-convergence and decrease the uncertainty associated with estimated diet proportions and PESCs. Therefore, we encourage future studies to use the spatio-temporal modelling framework developed by Grüss and Thorson (2019), which relies on a computationally efficient approximation to a compound Poisson-Gamma process, to estimate PESCs (and, subsequently, diet proportions) from a combination of prey biomass, prey count and prey occurrence data. Moreover, our spatio-temporal model could generate more accurate and more precise estimates in future studies if the degree of stomach fullness, differential digestion or gastric evacuation rates were taken into account (Ainsworth et al., 2010; Macdonald, Waiwood, & Green, 1982; Moriarty et al., 2017).

For simplicity, the spatio-temporal model developed in this study did not integrate environmental or catchability covariates. However, there are many instances where implementations of our model would benefit from including these covariates, either to improve the proportion of variability in the data explained by the model (in the case of environmental covariates) or to account for nuisance parameters (in the case of catchability covariates). Future studies implementing our spatio-temporal modelling approach could identify candidate environmental covariates based on the literature and expert opinion and select among those covariates using criteria such as Akaike's information criterion (Grüss et al., 2020; Moriarty et al., 2017; Thorson, 2015). Integrating catchability covariates into our spatio-temporal model may be particularly useful in situations where analysts have access to diet data that were collected using different fishing gear types. Combining diet data obtained using different gear types allows the sample size to be increased, but the effects of these different gear types must then be accounted for. For instance, gear types such as longlines and gill nets accumulate or entangle fish for a long time, meaning

that the stomachs of the fish collected in this manner generally contain a lot of prey items in an advanced state of digestion (Ainsworth et al., 2010; Baker et al., 2014; Cortés, 1997). Analysts can account for the effects of different gear types in our spatio-temporal model via a gear factor treated as a random effect through the implementation of restricted maximum likelihood (Grüss, Perryman, et al., 2018; Grüss, Thorson, et al., 2017, 2018).

In this study, we introduced a spatio-temporal modelling approach to estimating diet proportions and PESCs, and we also provided a roadmap for future spatio-temporal modelling efforts. In parallel, we encourage efforts to collect larger numbers of stomachs over larger spatial areas and longer periods of time in data-limited systems like the Gulf of Mexico, because this will be the only way to reveal meaningful spatio-temporal changes in fish diet patterns as exemplified in our demonstration for EBS large walleye pollock. Collecting more fish stomachs over larger spatial areas and longer periods will also reduce biases including the effects of order of ingestion and increase the probability of finding prey in stomachs that are not in an advanced digested state (Ainsworth et al., 2010; Baker et al., 2014; Binion-Rock et al., 2018). Increased sampling efforts would benefit from simulation experiments to identify the sampling designs that optimally utilize available resources, while understanding if and how sampling design specifics affect the performance of our spatio-temporal modelling approach (Reich, Pacifici, & Stallings, 2018; Thorson, 2019). In addition, sampling surveys that specifically target rare feeding events and juvenile predators are critically needed to fill in gaps in our understanding of fish diet patterns (Binion-Rock et al., 2018; Sagarese et al., 2016).

DATA AVAILABILITY STATEMENT

The biomass catch rate data collected by the SEAMAP (Southeast Area Monitoring and Assessment Program) groundfish trawl survey are available for download at: https://seamap.gsmfc.org/datarequests/index.php. The stomach content data collected by the Florida Fish and Wildlife Conservation Commission (FWC) are available

upon request to Dr. Kevin A. Thompson (Kevin.Thompson@myfwc.com). The biomass catch rate data collected within the standardized eastern Bering Sea bottom trawl surveys conducted by the Alaska Fisheries Science Center (AFSC) are available upon request to Dr. Stan Kotwicki (stan.kotwicki@noaa.gov). Finally, the stomach content data collected in the eastern Bering Sea region are available for download at: https://access.afsc.noaa.gov/REEM/WebDietData/DietDataIntro.php.

ORCID

Arnaud Grüss (iD) https://orcid.org/0000-0003-0124-6021
James T. Thorson (iD) https://orcid.org/0000-0001-7415-1010
Kirstin K. Holsman (iD) https://orcid.org/0000-0001-6361-2256
Stan Kotwicki (iD) https://orcid.org/0000-0002-6112-5021
Cameron H. Ainsworth (iD) https://orcid.org/0000-0001-5300-8290

REFERENCES

Ainsworth, C. H., Kaplan, I. C., Levin, P. S., & Mangel, M. (2010). A statistical approach for estimating fish diet compositions from multiple data sources: Gulf of California case study. *Ecological Applications*, *20*(8), 2188–2202. https://doi.org/10.1890/09-0611.1

Arreguín-Sánchez, F., Valero-Pacheco, E., & Chávez, E. A. (1993). *A trophic box model of the coastal fish communities of the southwestern Gulf of Mexico. Issue 26 of ICLARM Technical Reports*. Manila, Philippines: The WorldFish Center.

Aydin, K., & Mueter, F. (2007). The Bering Sea – A dynamic food web perspective. *Deep Sea Research Part II: Topical Studies in Oceanography*, *54*(23), 2501–2525. https://doi.org/10.1016/j.dsr2.2007.08.022

Baker, R., Buckland, A., & Sheaves, M. (2014). Fish gut content analysis: Robust measures of diet composition. *Fish and Fisheries*, *15*(1), 170–177. https://doi.org/10.1111/faf.12026

Barbeaux, S. (2018). Visualizations of groundfish distributions from Alaska Fisheries Science Center bottom trawl surveys. *Pacific States E-Journal of Scientific Visualizations*, https://doi.org/10.28966/PSESV.2018.001

Binion-Rock, S. M., Reich, B. J., & Buckel, J. A. (2018). A spatial kernel density method to estimate the diet composition of fish. *Canadian Journal of Fisheries and Aquatic Sciences*, *76*(2), 249–267. https://doi.org/10.1139/cjfas-2017-0306

Boldt, J. L., Buckley, T. W., Rooper, C. N., & Aydin, K. (2012). Factors influencing cannibalism and abundance of walleye pollock (*Theragra chalcogramma*) on the eastern Bering Sea shelf, 1982–20. *Fishery Bulletin*, *110*(3), 293–306.

Boldt, J., Rooper, C., & Hoff, J. (2015). Eastern Bering Sea groundfish condition. In S. Zador (Ed.), *Ecosystem considerations 2015 status of Alaska's marine ecosystems* (pp. 182–190). Anchorage, AK: North Pacific Fishery Management Council.

Bradley, E., & Bryan, C. E. (1975). *Life history and fishery of the red snapper (Lutjanus campechanus) in the northwestern Gulf of Mexico: 1970–1974*. Proceedings of the Gulf and Caribbean Fisheries Institute, pp. 77–106.

Brown, S. C., Bizzarro, J. J., Cailliet, G. M., & Ebert, D. A. (2012). Breaking with tradition: Redefining measures for diet description with a case study of the Aleutian skate *Bathyraja aleutica* (Gilbert 1896). *Environmental Biology of Fishes*, *95*(1), 3–20. https://doi.org/10.1007/s10641-011-9959-z

Buckley, T. W., Ortiz, I., Kotwicki, S., & Aydin, K. (2016). Summer diet composition of walleye pollock and predator–prey relationships with copepods and euphausiids in the eastern Bering Sea, 1987–2011. *Deep Sea Research Part II: Topical Studies in Oceanography*, *134*, 302–311. https://doi.org/10.1016/j.dsr2.2015.10.009

Carroll, G., Holsman, K. K., Brodie, S., Thorson, J. T., Hazen, E. L., Bograd, S. J., ... Selden, R. L. (2019). A review of methods for quantifying spatial predator–prey overlap. *Global Ecology and Biogeography*, *28*(11), 1561–1577. https://doi.org/10.1111/geb.12984

Catano, L. B., Shantz, A. A., & Burkepile, D. E. (2014). Predation risk, competition, and territorial damselfishes as drivers of herbivore foraging on Caribbean coral reefs. *Marine Ecology Progress Series*, *511*, 193–207. https://doi.org/10.3354/meps10921

Chagaris, D. D., Mahmoudi, B., Walters, C. J., & Allen, M. S. (2015). Simulating the trophic impacts of fishery policy options on the West Florida Shelf using Ecopath with Ecosim. *Marine and Coastal Fisheries*, *7*(1), 44–58. https://doi.org/10.1080/19425120.2014.966216

Charnov, E. L. (1976). Optimal foraging: Attack strategy of a mantid. *The American Naturalist*, *110*(971), 141–151. https://doi.org/10.1086/283054

Christensen, V., & Pauly, D. (1993). *Trophic models of aquatic ecosystems. Issue 26 of ICLARM Technical Reports*. Manila, Philippines: The WorldFish Center.

Christensen, V., & Walters, C. J. (2004). Ecopath with ecosim: Methods, capabilities and limitations. *Ecological Modelling*, *172*(2–4), 109–139. https://doi.org/10.1016/j.ecolmodel.2003.09.003

Coleman, F. C., Koenig, C. C., Scanlon, K. M., Heppell, S., Heppell, S., & Miller, M. W. (2010). Benthic habitat modification through excavation by red grouper, *Epinephelus morio*, in the northeastern Gulf of Mexico. *The Open Fish Science Journal*, *3*(1), 1–15. https://doi.org/10.2174/1874401X01003010001

Cortés, E. (1997). A critical review of methods of studying fish feeding based on analysis of stomach contents: Application to elasmobranch fishes. *Canadian Journal of Fisheries and Aquatic Sciences*, *54*(3), 726–738. https://doi.org/10.1139/f96-316

Daskalov, G. M. (2002). Overfishing drives a trophic cascade in the Black Sea. *Marine Ecology Progress Series*, *225*, 53–63. https://doi.org/10.3354/meps225053

Douma, J. C., & Weedon, J. T. (2019). Analyzing continuous proportions in ecology and evolution: A practical introduction to beta and Dirichlet regression. *Methods in Ecology and Evolution*, https://doi.org/10.1111/2041-210X.13234

Dwyer, D. A., Bailey, K. M., & Livingston, P. A. (1987). Feeding habits and daily ration of walleye pollock (*Theragra chalcogramma*) in the eastern Bering Sea, with special reference to cannibalism. *Canadian Journal of Fisheries and Aquatic Sciences*, *44*(11), 1972–1984. https://doi.org/10.1139/f87-242

Eisner, L. B., Napp, J. M., Mier, K. L., Pinchuk, A. I., & Andrews, A. G. III (2014). Climate-mediated changes in zooplankton community structure for the eastern Bering Sea. *Deep Sea Research Part II: Topical Studies in Oceanography*, *109*, 157–171. https://doi.org/10.1016/j.dsr2.2014.03.004

Elliott, J. M., & Persson, L. (1978). The estimation of daily rates of food consumption for fish. *Journal of Animal Ecology*, *47*(3), 977–991. https://doi.org/10.2307/3682

Fitzhugh, G. R., Lyon, H. M., Walling, W. T., Levins, C. F., & Lombardi-Carlson, L. A. (2006). *An update of Gulf of Mexico red grouper reproductive data and parameters for SEDAR 12. SEDAR 12-DW04*. North Charleston, SC: SEDAR, 18 pp.

Francis, R. C. (2011). Data weighting in statistical fisheries stock assessment models. *Canadian Journal of Fisheries and Aquatic Sciences*, *68*(6), 1124–1138. https://doi.org/10.1139/f2011-025

Froese, R., & Pauly, D. (2019). *FishBase*. World Wide Web Electronic Publication. Retrieved from www.fishbase.org

Fulton, E. A., Link, J. S., Kaplan, I. C., Savina-Rolland, M., Johnson, P., Ainsworth, C., ... Smith, D. C. (2011). Lessons in modelling and management of marine ecosystems: The Atlantis experience. *Fish and Fisheries*, *12*(2), 171–188. https://doi.org/10.1111/j.1467-2979.2011.00412.x

Fulton, E. A., Parslow, J. S., Smith, A. D., & Johnson, C. R. (2004). Biogeochemical marine ecosystem models II: The

effect of physiological detail on model performance. *Ecological Modelling*, *173*(4), 371–406. https://doi.org/10.1016/j.ecolm odel.2003.09.024

GCOOS (Gulf of Mexico Coastal Observing System). (2018, April 20). *Coastal Relief Model for the Gulf of Mexico*. Retrieved from http://gcoos.tamu.edu/products/topography/CRM.html

Geers, T. M., Pikitch, E. K., & Frisk, M. G. (2016). An original model of the northern Gulf of Mexico using Ecopath with Ecosim and its implications for the effects of fishing on ecosystem structure and maturity. *Deep Sea Research Part II: Topical Studies in Oceanography*, *129*, 319–331. https://doi.org/10.1016/j.dsr2.2014.01.009

Glaser, S. M. (2010). Interdecadal variability in predator–prey interactions of juvenile North Pacific albacore in the California Current System. *Marine Ecology Progress Series*, *414*, 209–221. https://doi.org/10.3354/meps08723

Grüss, A., Gao, J., Thorson, J. T., Rooper, C. N., Thompson, G., Boldt, J. L., & Lauth, R. (2020). Estimating synchronous changes in condition and density in eastern Bering Sea fishes. *Marine Ecology Progress Series*, *635*, 169–185. https://doi.org/10.3354/meps13213

Grüss, A., Perryman, H. A., Babcock, E. A., Sagarese, S. R., Thorson, J. T., Ainsworth, C. H., … Switzer, T. S. (2018). Monitoring programs of the US Gulf of Mexico: Inventory, development and use of a large monitoring database to map fish and invertebrate spatial distributions. *Reviews in Fish Biology and Fisheries*, *28*, 667–691. https://doi.org/10.1007/s11160-018-9525-2

Grüss, A., Rose, K. A., Simons, J., Ainsworth, C. H., Babcock, E. A., Chagaris, D. D., … Zetina Rejon, M. J. (2017). Recommendations on the use of ecosystem modeling for informing ecosystem-based fisheries management and restoration outcomes in the Gulf of Mexico. *Marine and Coastal Fisheries*, *9*(1), 281–295. https://doi.org/10.1080/19425 120.2017.1330786

Grüss, A., Schirripa, M. J., Chagaris, D., Velez, L., Shin, Y.-J., Verley, P., … Ainsworth, C. H. (2016). Estimating natural mortality rates and simulating fishing scenarios for Gulf of Mexico red grouper (*Epinephelus morio*) using the ecosystem model OSMOSE-WFS. *Journal of Marine Systems*, *154*, 264–279. https://doi.org/10.1016/j.jmars ys.2015.10.014

Grüss, A., & Thorson, J. T. (2019). Developing spatio-temporal models using multiple data types for evaluating population trends and habitat usage. *ICES Journal of Marine Science*, *76*(6), 1748–1761. https://doi.org/10.1093/icesjms/fsz075

Grüss, A., Thorson, J. T., Babcock, E. A., & Tarnecki, J. H. (2018). Producing distribution maps for informing ecosystem-based fisheries management using a comprehensive survey database and spatio-temporal models. *ICES Journal of Marine Science*, *75*(1), 158–177. https://doi.org/10.1093/icesjms/fsx120

Grüss, A., Thorson, J. T., Sagarese, S. R., Babcock, E. A., Karnauskas, M., Walter, J. F. III, & Drexler, M. (2017). Ontogenetic spatial distributions of red grouper (*Epinephelus morio*) and gag grouper (*Mycteroperca microlepis*) in the US Gulf of Mexico. *Fisheries Research*, *193*, 129–142. https://doi.org/10.1016/j.fishres.2017.04.00

Holsman, K. K., Ianelli, J., Aydin, K., Punt, A. E., & Moffitt, E. A. (2016). A comparison of fisheries biological reference points estimated from temperature-specific multi-species and single-species climate-enhanced stock assessment models. *Deep Sea Research Part II: Topical Studies in Oceanography*, *134*, 360–378. https://doi.org/10.1016/j.dsr2.2015.08.001

Hunsicker, M. E., Ciannelli, L., Bailey, K. M., Zador, S., & Stige, L. C. (2013). Climate and demography dictate the strength of predator-prey overlap in a subarctic marine ecosystem. *PLoS ONE*, *8*(6), e66025. https://doi.org/10.1371/journal.pone.0066025

Hunt, G. L., Stabeno, P. J., Strom, S., & Napp, J. M. (2008). Patterns of spatial and temporal variation in the marine ecosystem of the southeastern Bering Sea, with special reference to the Pribilof Domain.

Deep Sea Research Part II: Topical Studies in Oceanography, *55*(16), 1919–1944. https://doi.org/10.1016/j.dsr2.2008.04.032

Hynes, H. B. N. (1950). The food of fresh-water sticklebacks (*Gasterosteus aculeatus* and *Pygosteus pungitius*), with a review of methods used in studies of the food of fishes. *The Journal of Animal Ecology*, *19*, 36–58. https://doi.org/10.2307/1570

Hyslop, E. J. (1980). Stomach contents analysis – A review of methods and their application. *Journal of Fish Biology*, *17*(4), 411–429. https://doi.org/10.1111/j.1095-8649.1980.tb02775.x

Ianelli, J. N., Kotwicki, S., Honkalehto, T., McCarthy, A., Stienessen, S., Holsman, H., … Fissel, B. (2018). Chapter 1: Assessment of the walleye pollock stock in the Eastern Bering Sea. *Stock assessment and fishery evaluation report for the groundfish resources of the Bering Sea/Aleutian Islands regions* (pp. 1–155). Seattle, WA: Alaska Fisheries Science Center, National Marine Fisheries Service.

Kaplan, I. C., Francis, T. B., Punt, A. E., Koehn, L. E., Curchitser, E., Hurtado-Ferro, F., … Levin, P. S. (2019). A multi-model approach to understanding the role of Pacific sardine in the California Current food web. *Marine Ecology Progress Series*, *617–618*, 307–321. https://doi.org/10.3354/meps12504

Kass, R. E., & Steffey, D. (1989). Approximate Bayesian inference in conditionally independent hierarchical models (parametric empirical Bayes models). *Journal of the American Statistical Association*, *84*, 717–726. https://doi.org/10.2307/2289653

Kelleher, K. (2005). *Discards in the world's marine fisheries: An update. FAO Fisheries Technical Paper. No. 470*. Rome, Italy: FAO.

Kinzey, D., & Punt, A. E. (2009). Multispecies and single-species models of fish population dynamics: Comparing parameter estimates. *Natural Resource Modeling*, *22*(1), 67–104. https://doi.org/10.1111/j.1939-7445.2008.00030.x

Koehn, L. E., Essington, T. E., Marshall, K. N., Kaplan, I. C., Sydeman, W. J., Szoboszlai, A. I., & Thayer, J. A. (2016). Developing a high taxonomic resolution food web model to assess the functional role of forage fish in the California Current ecosystem. *Ecological Modelling*, *335*, 87–100. https://doi.org/10.1016/j.ecolmodel.2016.05.010

Kotwicki, S., Buckley, T. W., Honkalehto, T., & Walters, G. (2005). Variation in the distribution of walleye pollock (*Theragra chalcogramma*) with temperature and implications for seasonal migration. *Fishery Bulletin*, *103*(4), 574–587.

Kristensen, K., Nielsen, A., Berg, C. W., Skaug, H., & Bell, B. (2016). TMB: Automatic differentiation and Laplace approximation. *Journal of Statistical Software*, *70*, 1–20. https://doi.org/10.18637/jss.v070.i05

Liao, H., Pierce, C. L., & Larscheid, J. G. (2001). Empirical assessment of indices of prey importance in the diets of predacious fish. *Transactions of the American Fisheries Society*, *130*(4), 583–591. https://doi.org/10.1577/1548-8659(2001)130<0583:EAOIOP>2.0.CO;2

Lilly, G. R., Parsons, D. G., & Kulka, D. W. (2000). Was the increase in shrimp biomass on the northeast Newfoundland shelf a consequence of a release in predation pressure from cod? *Journal of Northwest Atlantic Fishery Science*, *27*, 45–62. https://doi.org/10.2960/J.v27.a5

Lindgren, F., Rue, H., & Lindström, J. (2011). An explicit link between Gaussian fields and Gaussian Markov random fields: The stochastic partial differential equation approach. *Journal of the Royal Statistical Society: Series B (Statistical Methodology)*, *73*, 423–498. https://doi.org/10.1111/j.1467-9868.2011.00777.x

Livingston, P. A., Aydin, K., Buckley, T. W., Lang, G. M., Yang, M.-S., & Miller, B. S. (2017). Quantifying food web interactions in the North Pacific – A data-based approach. *Environmental Biology of Fishes*, *100*(4), 443–470. https://doi.org/10.1007/s10641-017-0587-0

Livingston, P. A., & Jurado-Molina, J. (2000). A multispecies virtual population analysis of the eastern Bering Sea. *ICES Journal of Marine Science*, *57*(2), 294–299. https://doi.org/10.1006/jmsc.1999.0524

Livingston, P. A., Ward, A., Lang, G. M., & Yang, M.-S. (1993). *Groundfish food habits and predation on commercially important prey species in the*

eastern Bering Sea from 1987 to 1989. U.S. Department of Commerce, NOAA Technical Memorandum, NMFS-AFSC-11, 192 pp.

Lo, N. C., Jacobson, L. D., & Squire, J. L. (1992). Indices of relative abundance from fish spotter data based on delta-lognornial models. *Canadian Journal of Fisheries and Aquatic Sciences*, 49(12), 2515–2526. https://doi.org/10.1139/f92-278

Lombardi-Carlson, L., Fitzhugh, G., Palmer, C., Gardner, C., Farsky, R., & Ortiz, M. (2008). Regional size, age and growth differences of red grouper (*Epinephelus morio*) along the west coast of Florida. *Fisheries Research*, 91(2–3), 239–251. https://doi.org/10.1016/j.fishres.2007.12.001

Macdonald, J. S., Waiwood, K. G., & Green, R. H. (1982). Rates of digestion of different prey in Atlantic cod (*Gadus morhua*), ocean pout (*Macrozoarces americanus*), winter flounder (*Pseudopleuronectes americanus*), and American plaice (*Hippoglossoides platessoides*). *Canadian Journal of Fisheries and Aquatic Sciences*, 39(5), 651–659. https://doi.org/10.1139/f82-094

Masi, M. D., Ainsworth, C. H., & Chagaris, D. (2014). A probabilistic representation of fish diet compositions from multiple data sources: A Gulf of Mexico case study. *Ecological Modelling*, 284, 60–74. https://doi.org/10.1016/j.ecolmodel.2014.04.005

McCawley, J. R., Cowan, J. H. Jr, & Shipp, R. L. (2006). Feeding periodicity and prey habitat preference of red snapper, *Lutjanus campechanus* (Poey, 1860) on Alabama artificial reefs. *Gulf of Mexico Science*, 24(1), 14–27. https://doi.org/10.18785/goms.2401.04

Moriarty, P. E., Essington, T. E., & Ward, E. J. (2017). A novel method to estimate prey contributions to predator diets. *Canadian Journal of Fisheries and Aquatic Sciences*, 74(2), 168–177. https://doi.org/10.1139/cjfas-2016-0149

Morzaria-Luna, H. N., Ainsworth, C. H., Tarnecki, J. H., & Grüss, A. (2018). Diet composition uncertainty determines impacts on fisheries following an oil spill. *Ecosystem Services*, 33, 187–198. https://doi.org/10.1016/j.ecoser.2018.05.002

Nielsen, L. A., & Johnson, D. L., & American Fisheries Society. (1983). *Fisheries techniques*. Bethesda, MD: American Fisheries Society.

NOAA Fisheries. (2019, March 20). *Stomach content data collected in the eastern Bering Sea region*. Retrieved from https://access.afsc.noaa.gov/REEM/WebDietData/DietDataIntro.php

Northfield, T. D., Barton, B. T., & Schmitz, O. J. (2017). A spatial theory for emergent multiple predator–prey interactions in food webs. *Ecology and Evolution*, 7(17), 6935–6948. https://doi.org/10.1002/ece3.3250

O'Farrell, H., Grüss, A., Sagarese, S. R., Babcock, E. A., & Rose, K. A. (2017). Ecosystem modeling in the Gulf of Mexico: Current status and future needs to address ecosystem-based fisheries management and restoration activities. *Reviews in Fish Biology and Fisheries*, 27(3), 587–614. https://doi.org/10.1007/s11160-017-9482-1

Patrick, W. S., & Link, J. S. (2015). Myths that continue to impede progress in ecosystem-based fisheries management. *Fisheries*, 40(4), 155–160. https://doi.org/10.1080/03632415.2015.1024308

Pauly, D., Christensen, V., & Walters, C. (2000). Ecopath, Ecosim, and Ecospace as tools for evaluating ecosystem impact of fisheries. *ICES Journal of Marine Science*, 57(3), 697–706. https://doi.org/10.1006/jmsc.2000.0726

Pierce, G. J., & Boyle, P. R. (1991). A review of methods for diet analysis in piscivorous marine mammals. *Oceanography and Marine Biology*, 29, 409–486.

Pikitch, E., Boersma, P. D., Boyd, I., Conover, D., Cury, P., Essington, T., … Pauly, D. (2012). *Little fish, big impact: Managing a crucial link in ocean food webs*. Washington, DC: Lenfest Ocean Program.

Plagányi, É. E., & Essington, T. E. (2014). When the SURFs up, forage fish are key. *Fisheries Research*, 159, 68–74. https://doi.org/10.1016/j.fishres.2014.05.011

Reich, B. J., Pacifici, K., & Stallings, J. W. (2018). Integrating auxiliary data in optimal spatial design for species distribution modelling. *Methods in Ecology and Evolution*, 9(6), 1626–1637. https://doi.org/10.1111/2041-210X.13002

Rester, J. K. (2017). *SEAMAP environmental and biological atlas of the Gulf of Mexico, 2015. Number 263*. Gulf States Marine Fisheries Commission, Ocean Springs, MS, 72 pp.

Reum, J. C., Blanchard, J. L., Holsman, K. K., Aydin, K., & Punt, A. E. (2019). Species-specific ontogenetic diet shifts attenuate trophic cascades and lengthen food chains in exploited ecosystems. *Oikos*, 128, 1051–1064. https://doi.org/10.1111/oik.05630

Rose, K. A., Sable, S., DeAngelis, D. L., Yurek, S., Trexler, J. C., Graf, W., & Reed, D. J. (2015). Proposed best modeling practices for assessing the effects of ecosystem restoration on fish. *Ecological Modelling*, 300, 12–29. https://doi.org/10.1016/j.ecolmodel.2014.12.020

Sagarese, S. R., Nuttall, M. A., Geers, T. M., Lauretta, M. V., Walter, J. F. III, & Serafy, J. E. (2016). Quantifying the trophic importance of Gulf menhaden within the northern Gulf of Mexico ecosystem. *Marine and Coastal Fisheries*, 8(1), 23–45. https://doi.org/10.1080/19425120.2015.1091412

Sagarese, S. R., Walter, J. F. III, Harford, W. J., Grüss, A., Stumpf, R. P., & Christman, M. C. (2018). *Updating indices of red tide severity for incorporation into stock assessments for the shallow-water grouper complex in the Gulf of Mexico. SEDAR61-WP-07*. North Charleston, SC: SEDAR, 12 pp.

Saltelli, A., Tarantola, S., Campolongo, F., & Ratto, M. (2004). *Sensitivity analysis in practice: A guide to assessing scientific models*. West Sussex, UK: Wiley.

SEAMAP. (2019, January 2). *SEAMAP (Southeast Area Monitoring and Assessment Program) groundfish trawl survey data*. Retrieved from https://seamap.gsmfc.org/datarequests/index.php

SEDAR. (2009). *Stock assessment of red grouper in the Gulf of Mexico. SEDAR Update Assessment*. Retrieved from http://www.sefsc.noaa.gov/sedar/

Selden, R. L., Batt, R. D., Saba, V. S., & Pinsky, M. L. (2018). Diversity in thermal affinity among key piscivores buffers impacts of ocean warming on predator–prey interactions. *Global Change Biology*, 24(1), 117–131. https://doi.org/10.1111/gcb.13838

Shelton, A. O., Thorson, J. T., Ward, E. J., & Feist, B. E. (2014). Spatial semiparametric models improve estimates of species abundance and distribution. *Canadian Journal of Fisheries and Aquatic Sciences*, 71, 1655–1666. https://doi.org/10.1139/cjfas-2013-0508

Shin, Y.-J., & Cury, P. (2001). Exploring fish community dynamics through size-dependent trophic interactions using a spatialized individual-based model. *Aquatic Living Resources*, 14(2), 65–80. https://doi.org/10.1016/S0990-7440(01)01106-8

Siddon, E., & Zador, S. (2018). *Ecosystem status report 2018: Eastern Bering Sea, stock assessment and fishery evaluation report. Stock Assessment and Fishery Evaluation Report for the North Pacific Fishery Management Council Bering Sea and Aleutian Islands*. Anchorage, AK: Alaska Fisheries Science Center, National Marine Fisheries Service.

Stauffer, G. (2004). *NOAA protocols for groundfish bottom trawl surveys of the nation's fishery resources*. U.S. Department of Commerce, NOAA Technical Memorandum NMFS-F/SPO-65, 205 pp.

Tarnecki, J. H., Wallace, A. A., Simons, J. D., & Ainsworth, C. H. (2016). Progression of a Gulf of Mexico food web supporting Atlantis ecosystem model development. *Fisheries Research*, 179, 237–250. https://doi.org/10.1016/j.fishres.2016.02.023

Thompson, K. A., Switzer, T. S., Christman, M. C., Keenan, S. F., Gardner, C., & Campbell, M. (2018). *Indices of abundance for Red Grouper (Epinephelus morio) using combined data from three independent video surveys. SEDAR61-WP-03*. North Charleston, SC: SEDAR, 18 pp.

Thorson, J. T. (2014). Standardizing compositional data for stock assessment. *ICES Journal of Marine Science*, 71(5), 1117–1128. https://doi.org/10.1093/icesjms/fst224

Thorson, J. T. (2015). Spatio-temporal variation in fish condition is not consistently explained by density, temperature, or season for

California Current groundfishes. *Marine Ecology Progress Series*, *526*, 101–112. https://doi.org/10.3354/meps11204

Thorson, J. T. (2018). Three problems with the conventional delta-model for biomass sampling data, and a computationally efficient alternative. *Canadian Journal of Fisheries and Aquatic Sciences*, *75*, 1369–1382. https://doi.org/10.1139/cjfas-2017-0266

Thorson, J. T. (2019). Guidance for decisions using the Vector Autoregressive Spatio-Temporal (VAST) package in stock, ecosystem, habitat and climate assessments. *Fisheries Research*, *210*, 143–161. https://doi.org/10.1016/j.fishres.2018.10.013

Thorson, J. T., & Haltuch, M. A. (2018). Spatio-temporal analysis of compositional data: Increased precision and improved workflow using model-based inputs to stock assessment. *Canadian Journal of Fisheries and Aquatic Sciences*, *76*(3), 401–414. https://doi.org/10.1139/cjfas-2018-0015

Thorson, J. T., Johnson, K. F., Methot, R. D., & Taylor, I. G. (2017). Model-based estimates of effective sample size in stock assessment models using the Dirichlet-multinomial distribution. *Fisheries Research*, *192*, 84–93. https://doi.org/10.1016/j.fishres.2016.06.005

Thorson, J. T., & Kristensen, K. (2016). Implementing a generic method for bias correction in statistical models using random effects, with spatial and population dynamics examples. *Fisheries Research*, *175*, 66–74. https://doi.org/10.1016/j.fishres.2015.11.016

Thorson, J. T., Shelton, A. O., Ward, E. J., & Skaug, H. J. (2015). Geostatistical delta-generalized linear mixed models improve precision for estimated abundance indices for West Coast groundfishes. *ICES Journal of Marine Science*, *72*, 1297–1310. https://doi.org/10.1093/icesjms/fsu243

Walters, C., Christensen, V., Walters, W., & Rose, K. (2010). Representation of multistanza life histories in Ecospace models for spatial organization of ecosystem trophic interaction patterns. *Bulletin of Marine Science*, *86*(2), 439–459.

Walters, C., Martell, S. J., Christensen, V., & Mahmoudi, B. (2008). An Ecosim model for exploring Gulf of Mexico ecosystem management options: Implications of including multistanza life-history models for policy predictions. *Bulletin of Marine Science*, *83*(1), 251–271.

Walters, C., Pauly, D., & Christensen, V. (1999). Ecospace: Prediction of mesoscale spatial patterns in trophic relationships of exploited ecosystems, with emphasis on the impacts of marine protected areas. *Ecosystems*, *2*(6), 539–554. https://doi.org/10.1007/s100219900101

SUPPORTING INFORMATION

Additional supporting information may be found online in the Supporting Information section.